PONTIFICIA UNIVERSIDAD CATÓLICA DEL PERÚ

PONTIFICIA
UNIVERSIDAD
CATÓLICA
DEL PERÚ

PONTIFICIA UNIVERSIDAD CATÓLICA DEL PERÚ

ESCUELA DE POSGRADO

MAESTRÍA EN INGENIERÍA MECATRÓNICA

"Tracking Controller Design for a Nonlinear Model of a Gantry Crane based on Dynamic Extension and Robustification"

Tesis para optar el grado de Magíster en Ingeniería Mecatrónica

Presentado por:

José Luis Zárate Moya

Asesores

Prof. Dr.-Ing. Johann Reger (TU Ilmenau - Alemania)

Prof. Dr. Dante Elías (PUCP – Lima, Perú)

Miembros del Jurado

Tafur Sotelo, Julio Cesar

Elías Giordano, Dante Ángel (Asesor)

Villota Cerna, Elizabeth Roxana

Lima, Febrero de 2015

Technische Universität Ilmenau
Fakultät für Maschinenbau

Masterarbeit

für Herrn   Jose Luis Zarate Moya

geboren   am 15.09.1976   in Peru
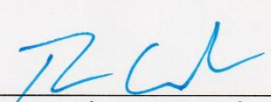
Studiengang   Mechatronik

THEMA

„Tracking Controller Design for a Nonlinear Model of a Gantry Crane based on Dynamic Extension and Robustification"

verantw. Hochschullehrer: Prof. Dr.-Ing. Johann Reger

Ausgabedatum: 01.08.2014   Abgabedatum: 02.02.2015

Ilmenau, den 10.09.2014

Prof. Dr.-Ing. Thomas Sattel
Studiengangverantwortlicher und Beauftragter
des Prüfungsausschusses für den Studiengang
Mechatronik

TECHNISCHE UNIVERSITÄT ILMENAU

Fakultät für Informatik und Automatisierung

Fachgebiet Regelungstechnik

Task Assignment of Master Thesis

B.Sc. José Luis Zárate Moya

Task: Tracking Controller Design for a Nonlinear Model of a Gantry Crane based on Dynamic Extension and Robustification

Gantry cranes are widely used for the transportation and positioning of heavy loads in logistic systems, e.g. at harbors or railway terminals. A major concern within application scenarios is to devise trajectories with minimal transition times. Another issue is to command feedback control signals that render the nominal transition less prone to oscillations before reaching the steady state. For solving these problems, among others, using an accurate nonlinear system model is indispensable. For the experimental gantry crane rig at the control laboratory of Control Engineering Group the nonlinear model of the system is a multiple-input multiple-output system that is input-state linearizable by means of dynamic feedback extension. In view of this property, the system has a so-called flat output by means of which an appropriate feed-forward signal may now be devised for solving the nominal tracking problem. The system in error coordinates then can be expressed as a linear time-invariant system of higher order. In this error system, lumped disturbances may serve to model both uncertainties and external disturbances. Consequently, for reducing the effect of the lumped disturbance on the tracking error it is natural to minimize the corresponding L_2-gain by means of an outer control loop. Thus, minimizing the H_∞-norm of the respective transfer function paves the way to a solution of the robust tracking problem.

The task of this master thesis is to revise and potentially correct a first Lagrangian-model of the gantry crane system, neglecting the actuator dynamics. In a next step, an input-state linearization of the nonlinear model is to be derived by means of an appropriate dynamic feedback extension. Based on the obtained linearization and the associated flat output, nominal feed-forward control signals shall be calculated for selected transition tasks that link given stationary set-points. The error dynamics shall then be controlled, first, by classical pole placement methods which are to be compared with LQR-based designs. These controllers finally shall be robustified using the Glover-McFarlane algorithm. For each of these settings, the closed-loop performance and robustness is to be studied and assessed via simulations.

Date of Issue: August 1, 2014
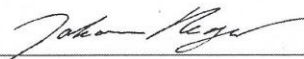
Supervisor at TU Ilmenau: Prof. Dr.-Ing. Johann Reger

Supervisor at PUCP/ Lima: Prof. Dr. Dante Elías
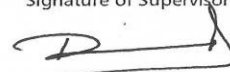
Ilmenau, 17th of July 2014
_____
Place and Date of Issue

_____
Signature of Supervisor at TU Ilmenau

Lima, September 5th, 2014
_____
Place and Date of Issue

_____
Signature of Supervisor at PUCP/ Lima

Ilmenau, August 27th, 2014
_____
Place and Date of Issue

_____
Signature of Student

Erklärung

Die vorliegende Arbeit habe ich selbstständig ohne Benutzung anderer als der angegebenen Quellen angefertigt. Alle Stellen, die wörtlich oder sinngemäß aus veröffentlichten Quellen entnommen wurden, sind als solche kenntlich gemacht. Die Arbeit ist in gleicher oder ähnlicher Form oder auszugsweise im Rahmen einer oder anderer Prüfungen noch nicht vorgelegt worden.

Ilmenau, den 02. 02. 2015   José Luis ZárateMoya

Kurzfassung

Kräne werden in der Industrie für den Transport schwerer Lasten eingesetzt. Man findet sie im Hochbau, Fabriken und Häfen. Traditionell werden sie von erfahrenen Kranführer betrieben. Das der Arbeit zugrunde liegende Kransystem besteht aus drei Hauptkomponenten: Transporteinheit, Brücke und Gerüst. Im Regelbetrieb ist das Schwingen von Krannutzlasten einer sicheren und effizienten Nutzung abträglich. Auch andere externe Störparameter wie beispielsweise der Wind haben einen Einfluss auf die Kontrollierbarkeit eines Krans. Grundsätzlich ist ein Kransystem ein unteraktuiertes System. Deshalb verkompliziert sich im Allgemeinen der Entwurf einer Regelung, meist auf Basis der Kranbeschleunigung. Regelziele bei der Kranbewegung sind u.a. eine hohe Positioniergenauigkeit, kurze Transportzeit, kleine Pendelwinkel und hohe Sicherheit. Das Hauptziel dieser Diplomarbeit ist der Entwurf einer robusten Reglung, gründend auf der H_∞-Regelungsttheorie, für ein nichtlineares Modell eines 3-D-Portalkran-Systems. Das Verfahren soll mit dem klassischen Controllerdesign verglichen und resultierende Regelungsprobleme infolge von Störungen im Nutzlasttransport untersucht werden. Das Modell beschreibt die Position der Last sowie deren zeitliche Ableitungen. Davon kann das Problem für den Entwurf einer flachheitsbasierten Vorsteuerung abgeleitet werden, die dann mit einer optimalen, linearen bzw. nichtlinearen Regelung verbunden wird. Die nominalen Zustände können als Optimierungsparameter und Beschränkungen für die Stabilität, Überschwingen, Positionsregelung und Schwingungswinkel verwendet werden, unabhängig von der Lastmaße und in Abhängigkeit von der Seillänge.

Dabei wird wie folgt vorgegangen: Zunächst wird ein nichtlineares Systemmodell mit Hilfe der Lagrange-Gleichungen erstellt. Dann wird das System mit Hilfe einer dynamischen Erweiterung exakt linearisiert. Als nächstes wird der geschlossene Regelkreis auf Basis der linear-quadratischen Regelung untersucht und mit einer robusten H_∞ Regelung zur Kompensation von Modellierungsfehlern oder systeminterner und -externe Störung verglichen. Schließlich werden Simulationsergebnisse vorgestellt, welche die Wirksamkeit des Entwurfes belegen. Ein Ergebnis st dabei die verbesserte Leistung des nichtlinearen Reglers gegenüber dem klassischen Regler. Dies wird anhand einer Fähigkeit zu Verfolgung einesr schnellen Bahn, der Präzision der Positionierung und der minimalen Einflussbewegung der Nutzlast dargestellt.

Abstract

Overhead cranes are widely used in industry for transportation of heavy loads and are common industrial structures used in building construction, factories, and harbors, traditionally operated by experienced crane operators. The underlyng system consists of three main components: trolley, bridge, and gantry. Basically, the system is a trolley with pendulum. In normal operation, the natural sway of crane payloads is detrimental to the safe and efficient action. Other external disturbances parameters, wind for example, also affect the controller performance. Basically, a crane system is an underactuated system. This makes the design of its controllers complicated. Usually, this is done via the crane acceleration required for motion. The most important issues in crane motion are high positioning accuracy, short transportation time, small sway angle, and high safety.

The main goal of this thesis is to achieve a robust controller design procedure, based on H_∞ control theory, for a nonlinear model of a 3-D gantry crane system. The approach shall be compared with classic controllers in terms of attenuating the perturbation on the payload transportation. The model describes the position of the load, as well as the time derivatives of the position. In vew of this, flatness-based feedforward control has to be devised, accompanied by the design of an optimal linear and nonlinear feedback controller. The nomnal states can be used as optimization parameters and restrictions on stability, overshoot, position regulation, and oscillation angle, being independent of the load mass and depending on the rope length.

The procedure is as follows. First, a dynamic nonlinear model of the system is obtained using the Lagrange equations of motion which describe the simultaneous travelling, crossing, lifting motions and the resultant load swing of the crane. Then, the system is exactly linearised by a dynamic extension. Next the closed-loop system, based on the linear quadratic regulator scheme, is probed and compared with the H_∞ robust control system for compensating modeling errors and/or internal and external perturbation. Finally, simulation results are presented showing the efficiency of the proposed controller design scheme. Results are provided to illustrate the improved performance of the nonlinear controllers over classic pole placement and linear quadratic regulator approaches, testing its fast input tracking capability, precise payload positioning and minimal sway motion.

Acknowledgment

The research included in this Master Thesis could not have been performed if not for the assistance, patience, and support of many individuals. I would like to extend my gratitude first and foremost to my thesis advisor Prof. Dr.-Ing. Johann Reger for mentoring me over the course of my master studies. I sincerely thank him for his confidence in me. I would additionally like to thank Prof. Dr.-Ing- Tom Ströhla, responsible for the dual degree program who has made possible this cooperation between Technische Universität Ilmenau and Pontificia Universidad Católica del Perú. I would also like to extend my appreciation to Prof. Dr. Dante Elías for his constant support and advice in all this years we have worked together in our research projects. This work would not have been possible without the support of DAAD and the double master program between both universities, giving the students the possibility to improve their knowledge and develop a shared cooperation among Peruvian and German students. Finally, I would like to extend my deepest gratitude to my family, Isabel, Eugenia and Gaudencia without whose love, support and understanding I could never have completed this master degree.

Abbreviations and Symbols

DOF	Degrees of freedom
SISO	Single Input, Single Output system
MIMO	Multiple Inputs, Multiple Outputs system
2-D	Two-dimensional space
3-D	Three-dimensional space
LTI	Linear time-invariant theory
LQR	Linear-quadratic regulator
PDE	Partial differential equation
T	Kinetic energy
P	Potential energy
L	Lagrangian of a dynamical system
Q	Euler–Lagrange equation of motion
C	Differentiable function class
K	State-feedback gain matrix
Q	Positive definite or semidefinite Hermitian Matrix
R	Positive definite Hermitian Matrix
M	Decoupling Matrix

Contents

List of Figures

List of Tables

1 Introduction

1.1 Motivation

The current direction of the modern industry is focused basically on improving the efficiency of the equipment involved in the work chain. Overhead cranes are widely used in industry and it is very important to ensure a good performance in order to save time, yield low cost, easy assembly and less maintenance and also reduce the risks during the transportation process. Three-dimensional (3-D) crane systems are usually found in airports, ports, and different industries. Its function is basically to carrying a heavy object to a desired position within a given time interval. These system, in essence, a cart with pendulum extension, have been developed and successfully employed in many practical setups until now.

The Gantry Crane system must be able to move to the desired positions as fast and as accurate as possible while positioning the payload at the suitable position. The exact positioning of a heavy load requires a skilled operator to estimate approximately the inertia of the carried mass to prevent overshoot of the load and to make smooth braking to reach the desired target position without load swing. The use of inexperienced operators can result in a large sway during the process of transportation of the load. Typically, this process is performed by an operator using only visual feedback to position the payload. It could exhibit a pendulum-like swinging motion especially when the payload is suddenly stopped after a fast motion. This may be dangerous and may cause damage and accidents. Furthermore, an overhead crane system may experience a range of parameter variations under different loading condition, for example, uncertainties of the load mass, different rope lengths and the constrained work area within manufacturing plants. For this reason, experience of the operator is important to move the load cautiously and slower than possible, while increasing transit times and reducing productivity. In general, human operators, assisted by qn automatic anti-sway system, are included in the operation of overhead crane systems. The combined performance, in terms of swiftness and safety, depends on their experience and efficiency, respectively. Therefore, the search of an appropriate control procedure in

the presence of external perturbations is a problem to solve.

In order to improve the efficiency of payload transportation, the trolley of a crane should move to its destination as quickly and as precisely as possible meanwhile the swing angle should be kept as small as possible, avoiding large payload swings during transport which may cause damage to the payload itself and surrounding equipment or personnel. Based on these requirements, motion planning has to be done requirng either planning a temporal trajectory along a predefined path or planning both a path and a trajectory.

Specifically, an overhead crane system is a representative underactuated system. This means that the number of inputs is less than the number of degrees of freedom with strong states coupling. The input signals applied to move the trolley generate a bi-axial sway motion on the load making difficult its displacement in a correct way. This kind of system is considered non-minimum phase if a nonlinear state feedback can hold the system output identically zero while the internal dynamics become unstable.

Due to the underactuation the principal challenge is to design a single control input to achieve the transport of the payload in a precise location as fast as possible without causing any excessive swing at the final position. This will need to take into consideration the uncertainties, for example, modelling and computation errors, unknown payloads, measurement noise, etc.

Different studies have been made to control the load swing. However, the nonlinear dynamic properties and the lack of actual control input for the sway motion might bring about undesired significant sway oscillations, especially, at take-off and arrival phases. Besides, in the presence of parametric and external perturbations, overhead cranes may present unstable zero dynamics, reducing the performance of the system.

Cranes are typically involved within complicated nonlinear systems. But for simplicity the model is usually approximated or linearized in order to be able to apply linear system theory for controller design. In addition, the height of the load is included in the control scheme making the controller account for hoisting and lowering of the load taking into consideration the reference velocity of the drive instead of the force as the available input of the system.

For this case, flatness-based control techniques have been developed and applied in many industrial processing with a great success in solving planning and tracking problems of reference trajectories applied on a crane control system. In this approach it is possible to express the state as well as the input and the output system as differential functions denominated flat output. Despite the effort to design a controller with good oscillation damping, the result often present a poor tracking behavior of the load

position.

The external disturbances that affects the payload in a controlled system can present lack of robustness in the trajectory tracking. For this reason, a common and effective solution in this kind of problems is the use of H_∞ control. The approach concerns the design of a stabilizing controller that minimizes the effects of the disturbances of the closed-loop system in the internal controller parameters. To increase performance it is necessary to include weighting functions in the minimization the H_∞ norm.

Several research on gantry crane systems and its control analysis have been studied previously. The theory shown in [BI90] about zero dynamics says it is possible to define a dynamic state feedback which renders a given nonlinear system locally diffeomorphic to a linear and controllable system if the system is invertible and the zero dynamics are trivial. They feature a 2-D Gantry Crane as an example for the solution of this kind of systems. This concept is further used in [CGZ05] and extended to partial feedback linearization to build a nonlinear controller for the gantry crane system. Another concept is related of the flatness-based control in [SMD]. In this case, the crane is modeled by a flat system by means of which the tracking controller has been constructed. The general concept of flat systems is exposed in the papers [FLMR95] and [MMR01] explaining that the Flat systems are a generalization of linear systems, but the techniques used for its control are different than many of the used techniques for linear systems. The terminology flat is due to the fact that the system output plays in the same analogous role to the flat coordinates in the differential geometric approach to the Frobenius theorem. With respect to the control of the crane, the work made in [BN92] present linearization techniques consisting in adaptive dynamic feedback control, considering the system as a completely controllable system. That is, they consider a classical rigid manipulator whose each degree of freedom is directly controlled. This led to end up with a simple pendulum of a punctual mass linked to a completely controlled system that is able to rotate with one or two degrees of freedom. In the works of [Yan09] and [CL08] the implementation of adaptive control is presented with a focus on the minimization of the sway and mass perturbation, respectively. A novel aproach of adaptive tracking control is studied in [YS11]. It is based on the notions of linear-in-parameter property and regressor matrices. The concept of controlling time derivatives in order to approach a controller design for a crane by generalized states variables is presented in [FLR91]. [Lee98] proposes to consider the load swing, crane motion, and load hoisting of a gantry crane within the modeling and control. This includes a new two-degree-of freedom swing angle, making equivalent a three-link flexible robot having the first flexible mode to find a control of the system. The authors

of [KKS10] derived a model of the three dimensional overhead crane which imposes the desired trolley velocity in *x* and *y* direction and the desired hoisting velocity as the system input, assuming a first order approximation of the drive dynamics, in this crane system, the controller, based in Pole Placement method obtained of the resulting integrator chain, is independent of the load or trolley mass. According to [XW12] and [YLL14] the formulation of an optimal control problem for a gantry crane system in which both the linear feedback gain and the nonlinear feedback gain are tuned by solving a parameter optimization problem is possible through an ''optimal composite nonlinear feedback control law' based on the model of the gantry crane system and the form of the nonlinear function. Using a set of segmented transition polynomials for solving multi-point boundary value problems analytically for the movement of a 3-DOF gantry crane is implemented in [RKS11]. The paper of [VFC13] develops a second order sliding mode controller design that s based on the super-twisting controller for reducing external perturbations. An other type of sliding mode control is explained in [AZ09], using five highly nonlinear second-order ordinary differential equations with the implementation of a Luenberger-type observer to estimate the states of the 3-D overhead crane. With respect to nonlinear control concepts the article [FDDZ03] illustrates how nonlinear feedback terms may be incorporated within the controller design on order to provide additional feedback for the unactuated payload angle through the natural coupling between the gantry and the payload. Related to the robustification of the gantry crane systems, the work [ZPS12] presents a controller design that is based on H_∞ control using the concepts of Lyapunov and G-Shaping paradigms. The authors of [PPB] introduce two techniques for robustification, Glover-McFarlane H_∞ design and the two-degree of freedom controller design, and compare the efects of each one in terms of performance of a 3-D overhead crane. An other concept envolves H_∞ theory, as seen in [HPS13], where the reduced-order multi-objective H_∞ control problem for a discrete-time LTI dynamics is considered. They result in controllers with a high reliability and low implementation costs. The work made in [CLLL08] propose a robustification using Lyapunov-based model reference controller design via an additionally auxiliary control scheme for compensating the system error. This involves the use of an approximation based on model reference adaptive control algorithm. Aditionally, the work in [ZTMS$^+$13] explains the implementation of H_∞ controllers with linear matrix inequalities (LMI) and focuses on good time response specifications and closed-loop damping of an underactuated crane system forcing the closed-loop poles to the left-half plane.

This master thesis presents the analysis of a control system of a gantry crane system

with robustification, making a comparison between classic controllers like Pole Placement and LQR. To this end, the behaviour of these solutions is investigated to minimize the internal and external perturbations employing the concepts of flatness-based control of the gantry crane on the unactuated system, not depending on the mass. This work is based on a preliminary study entitled *Flachheitsbasierter Regelungsentwurf für einen Portalkran mit anschließender Robustifikation durch H∞ loop-shaping* manual [Jah13] of the Laboratory of Control and System Engineering 3 developed by Research Assistant Benjamin Jahn.

The thesis is organized as follows: In Chapter 2 a first Lagrangian model of the gantry crane system is developed, neglecting the actuator dynamics in order to obtain the nonlinear system equation. In Chapter 3 an input-state linearization of the nonlinear model is calculated using a suitable dynamic feedback extension. Based on the obtained linearization and the associated flat output, nominal feed-forward control signals shall be calculated in Chapter 4, then the system is controlled using the error dynamics by classical pole placement methods and is compared with LQR based designs. These controllers are finally robustified using the Glover-McFarlane algorithm. The simulation of the system is shown in Chapter 5 and eventually the conclusions are presented in Chapter 6.

2 Nonlinear Model of the Gantry Crane System

2.1 Modeling

In the following, a non-linear model of the dynamics of the three-dimensional gantry crane system is derived. To illustrate the observed kinematics, a schematic drawing of the three-dimensional gantry crane is shown in Figure 2.1. As can be readily seen, the trolley can only move in the $x - y$ plane, where $x_c(t)$ and $y_c(t)$ are the position of the trolley in the x and y coordinates, respectively. Therefore, we have

$$r_t(t) = \begin{bmatrix} \dot{x}_c(t) & \dot{y}_c(t) & 0 \end{bmatrix}^{\mathrm{T}}. \tag{2.1}$$
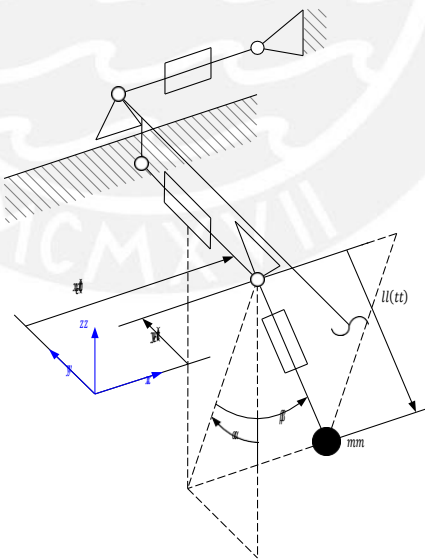

Figure 2.1: Schematics of three-dimensional overhead crane.

With respect to the schematic above, the following position for the mass point of the

load is obtained:

$$r_l(t) = \begin{bmatrix} x_c(t) + l(t)\sin(\beta(t)) \\ y_c(t) + \cos(\beta(t))l(t)\sin(\alpha(t)) \\ -l(t)\cos(\alpha(t))\cos(\beta(t)) \end{bmatrix}. \quad (2.2)$$

The dynamics of the gantry crane is to be derived using Lagrange's equations. Thus, it is necessary to establish the Lagrange function as the difference between kinetic and potential energy. The kinetic energy of the gantry crane is calculated from the sum of the kinetic energies of the trolley and the load, i.e.

$$T(\dot{r}_t, \dot{r}_l) = \frac{1}{2}m_t\dot{r}_t^{\mathrm{T}}\dot{r}_t + \frac{1}{2}m_l\dot{r}_l^{\mathrm{T}}\dot{r}_l = T(\dot{x}_t, \dot{y}_c, l, \dot{l}, q, \dot{q}). \quad (2.3)$$

The potential energy due to gravity $\bar{g} = [0\ 0\ g]^{\mathrm{T}}$ is calculated as follows

$$V(r_l) = m_l\bar{g}^{\mathrm{T}}r_l = -m_l g l \cos(\beta)\cos(\alpha) = V(l, q). \quad (2.4)$$

Using the Lagrange function $L = T - P$ the equations of motion of the gantry crane result from Lagrange's equations of the second kind where Q is the generalized forces which are determined by the projection of the external forces along the directions of the generalized coordinates.

$$\frac{d}{dt}\left[\frac{\partial L}{\partial \dot{q}}\right] - \frac{\partial L}{\partial q} = Q. \quad (2.5)$$

2.2 Transformation of the Underactuated Model of the Crane

Based on the solutions of [Lee98] and [AZ09] the crane model resulting from (2.5) may be represented as

$$\mathbf{M}(q)\ddot{q} + \mathbf{C}(q, \dot{q})\dot{q} + \mathbf{G}(q) = \mathbf{F} \quad (2.6)$$

which is the model of an underactuated system.

Generally, controlling an underactuated systems is considered complicated. Hence, the nonlinear model of the 3-D overhead crane system will be written in a form that is more appropriate for the design of controllers for underactuated systems.

The inputs of the system are f_x, f_y and f_l. Therefore, the number of inputs is $n_i = 3$. Clearly, the number of degrees of freedom of the crane system is $n_i = 5$. We separate

the states of the system into two vectors: actuated states q_1 and unactuated states q_2. Define the vectors q_1, q_2 and the force vector $\mathbf{F}_1$ as follows:

$$q_1 = \begin{bmatrix} x_c \\ y_c \\ l \end{bmatrix} , \quad q_2 = \begin{bmatrix} \alpha \\ \beta \end{bmatrix} , \quad \mathbf{F}_1 = \begin{bmatrix} f_x \\ f_y \\ t_l \end{bmatrix}.$$

Then the equations of motion of the 3-D overhead crane may be written as

$$\mathbf{M}_{11}(q)\ddot{q}_1 + \mathbf{M}_{12}(q)\ddot{q}_2 + \mathbf{C}_{11}(q,\dot{q})\dot{q}_1 + \mathbf{C}_{12}(q,\dot{q})\dot{q}_2 + \mathbf{G}_1(q) = \mathbf{F}_1 \tag{2.7a}$$

$$\mathbf{M}_{21}(q)\ddot{q}_1 + \mathbf{M}_{22}(q)\ddot{q}_2 + \mathbf{C}_{21}(q,\dot{q})\dot{q}_1 + \mathbf{C}_{22}(q,\dot{q})\dot{q}_2 + \mathbf{G}_2(q) = 0 \tag{2.7b}$$

where the matrices that form the system are

$$\mathbf{M}(q) = \begin{bmatrix} \mathbf{M}_{11}(q) & \mathbf{M}_{12}(q) \\ \mathbf{M}_{21}(q) & \mathbf{M}_{22}(q) \end{bmatrix} \tag{2.8}$$

$$\mathbf{C}(q,\dot{q}) = \begin{bmatrix} \mathbf{C}_{11}(q,\dot{q}) & \mathbf{C}_{12}(q,\dot{q}) \\ \mathbf{C}_{21}(q,\dot{q}) & \mathbf{C}_{22}(q,\dot{q}) \end{bmatrix} \tag{2.9}$$

$$\mathbf{G}(q) = \begin{bmatrix} \mathbf{G}_1(q) \\ \mathbf{G}_1(q) \end{bmatrix} \tag{2.10}$$

with

$$\mathbf{M}_{11}(q) = \begin{bmatrix} m_c + m_l & 0 & m_l \sin(\beta) \\ 0 & m_c + m_l & m_l \cos(\beta)\sin(\alpha) \\ m_l \sin(\beta) & m_l \cos(\beta)\sin(\alpha) & m_l \end{bmatrix}$$

$$\mathbf{M}_{12}(q) = \begin{bmatrix} 0 & m_l l \cos(\beta) \\ m_l l \cos(\alpha)\cos(\beta) & -m_l l \sin(\alpha)\sin(\beta) \end{bmatrix}$$

$$\mathbf{M}_{21}(q) = \begin{bmatrix} 0 & m_l l \cos(\alpha)\cos(\beta) & 0 \\ m_l l \cos(\beta) & -m_l l \sin(\alpha)\sin(\beta) & 0 \end{bmatrix}$$

$$\mathbf{M}_{22}(q) = \begin{bmatrix} m_l l^2 \cos^2(\beta) & 0 \\ 0 & m_l l^2 \end{bmatrix}$$

$$\mathbf{C}_{11}(q,\dot{q})=\begin{bmatrix} 0 & 0 & 2m_l\dot{\beta}\cos(\beta) \\ 0 & 0 & -2m_l\dot{\beta}\sin(\alpha)\sin(\beta)-\dot{\alpha}\cos(\alpha)\cos(\beta) \\ 0 & 0 & 0 \end{bmatrix}$$

$$\mathbf{C}_{12}(q,\dot{q})=\begin{bmatrix} 0 & -m_l l\dot{\beta}\sin(\beta) \\ -m_l l\dot{\alpha}\cos(\beta)\sin(\alpha) & -m_l l\dot{\beta}\cos(\beta)\sin(\alpha) \\ -m_l l\dot{\alpha}\cos^2(\beta) & -m_l l\dot{\beta} \end{bmatrix}$$

$$\mathbf{C}_{21}(q,\dot{q})=\begin{bmatrix} 0 & 0 & 2m_l l\dot{\alpha}\cos^2(\beta) \\ 0 & 0 & 2m_l l\dot{\beta} \end{bmatrix}$$

$$\mathbf{C}_{22}(q,\dot{q})=\begin{bmatrix} 0 & 0 \\ m_l l^2\dot{\alpha}\cos(\beta)\sin(\beta) & 0 \end{bmatrix}$$

$$\mathbf{G}_1(q)=\begin{bmatrix} 0 \\ 0 \\ -m_l g\cos(\alpha)\cos(\beta) \end{bmatrix}$$

$$\mathbf{G}_2(q)=\begin{bmatrix} m_l g l\sin(\alpha)\cos(\beta) \\ m_l g l\cos(\alpha)\sin(\beta) \end{bmatrix}$$

Clearly, $\mathbf{M}_{22}(q)$ is a positive-definite matrix for $l > 0$ and $\beta < \pi/2$. Then, by using equation (2.7b) we obtain

$$\ddot{q}_2 = -\mathbf{M}_{22}^{-1}(q)[\mathbf{M}_{21}(q)\ddot{q}_1 + \mathbf{C}_{21}(q,\dot{q})\dot{q}_1 + \mathbf{C}_{22}(q,\dot{q})\dot{q}_2 + \mathbf{G}_2(q)]. \qquad (2.11)$$

Following [KKS10] we work now with equation (2.11) in order to build the nonlinear model of the system. Considering $u = [\ddot{x}_c(t)\ \ddot{y}_c(t)\ \ddot{l}(t)]$ as the new inputs of the system, we obtain the equations of moment independent of the mass:

$$\ddot{\alpha} = \frac{1}{l\cos(\beta)}(2l\dot{\alpha}\dot{\beta}\sin(\beta) - g\sin(\alpha) - 2\dot{l}\dot{\alpha} - \cos(\alpha)\ddot{y}_c) \qquad (2.12a)$$

$$\ddot{\beta} = \frac{1}{l}(-g\cos(\alpha)\sin(\beta) - 2\dot{l}\dot{\beta} - l\dot{\alpha}^2\sin(\beta)(\cos(\beta)) - \cos(\beta)\ddot{x}_c + \sin(\alpha)\sin(\beta)\ddot{y}_c). \qquad (2.12b)$$

3 Linearization of the Gantry Crane System

3.1 Existence Conditions

The following basic concepts are drawn from the results exposed previously in [RPK13]. The type of nonlinear systems considered are represented by equations of the form:

$$\dot{x}(t) = f(x(t)) + \sum_{i=1}^{m} g_i(x(t))u_i(t). \tag{3.1}$$

A system with ths form is said to be affine. It is assumed that the vector fields f, g_1, $g_1,...,g_m$ are smooth differentiable mappings $R^n \rightarrow R^n$. These mappings are understood as n-dimensional real functions of the state variables $x_1, x_2,...,x_n$:

$$f(x(t)) = \begin{bmatrix} f_1(x_1(t), x_2(t), \cdots, x_n(t)) \\ f_2(x_1(t), x_2(t), \cdots, x_n(t)) \\ \vdots \\ f_n(x_1(t), x_2(t), \cdots, x_n(t)) \end{bmatrix} \tag{3.2}$$

$$g_i(x(t)) = \begin{bmatrix} g_{i1}(x_1(t), x_2(t), \cdots, x_n(t)) \\ g_{i2}(x_1(t), x_2(t), \cdots, x_n(t)) \\ \vdots \\ g_{in}(x_1(t), x_2(t), \cdots, x_n(t)) \end{bmatrix} \tag{3.3}$$

associated to an output

$$y_j = h_j(x(t)) \; 1 \leq j \leq p \,. \tag{3.4}$$

The functions $h_1, \ldots, h_p$: $R^n \rightarrow R$, characterize the system outputs as real functions of the state variables x_i. They shall be assumed smooth scalar functions and may be chosen by the designer, considering the possibilities of accessibility and measurements.

3.2 Feedback linearization for SISO systems

In the case when $m = 1$, system (3.1) to (3.4) are said to have relative degree r at a point $x_0 \in \mathsf{R}^n$ if $L_g h(x) = L_g L_f h(x) = \ldots = L_g L_f^{r-2} h(x) = 0$ in an open neighborhood of x_0 and $L_g L_f^{r-1} h(x_0) \neq 0$, shown in [Isi95]. System (3.1) is called exactly (feedback) linearizable if there exists a scalar field $\lambda : \mathsf{R}^n \rightarrow \mathsf{R}$ (acting as a virtual output) such that the resulting system has relative degree n, that is

$$L_g \lambda(x) = L_g L_f \lambda(x) = \cdots = L_g L_f^{r-2} \lambda(x) = 0, \; L_g L_f^{r-1} \lambda(x) = 0 \qquad (3.5)$$

holds for all x in a neighborhood of x_0. Such an output $\lambda = \lambda(x)$ is called a flat output [FLMR95].

It has been established that a single-input system (3.1) is exactly transformable into a controllable linear system if and only if the system is (differentially) flat [MMR01]. Using standard operations from differential geometry it can be shown that (3.5) is equivalent to the condition

$$L_g \lambda(x) = 0, \ldots, L_{ad_{-f}^{n-2} g} \lambda(x) = 0, L_{ad_{-f}^{n-1} g} \lambda(x) = 0 \qquad (3.6)$$

for all x in a neighborhood of x_0. The first $n - 1$ equations occurring in (3.6) can be written as first order partial differential equation (PDE)

$$d\lambda(x) \cdot \left[g(x), ad_{-f} g(x), \ldots, ad_{-f}^{n-2} g(x) \right] = 0^{\mathrm{T}}. \qquad (3.7)$$

Therefore, the existence of a flat output λ is directly linked to the existence of a nontrivial solution of (3.7). The existence of a nontrivial solution of (3.7) can be guaranteed using Frobenius' Theorem. This leads to a result obtained by Witold Respondek in 1980, see [Res02]:

Theorem 1: System (3.1) for $m = 1$ is exactly transformable into a controllable linear system in a neighborhood of $x_0 \in \mathsf{R}^n$ if and only if

1) the generalized controllability matrix

$$R(x_0) := \left[g(x_0), ad_{-f} g(x_0), \ldots, ad_{-f}^{n-1} g(x_0) g(x_0) \right] \qquad (3.8)$$

has rank n, and

2) the distribution $span\{g, ad_{-f}g, \ldots, ad_f^{n-2} g\}$ is involutive in a neighborhood of x_0.

If system (3.1) for $m = 1$ has the above properties and, thus is exactly linearizable,

then there exists a flat output. With a diffeomorphism and input transform

$$z = \mathbf{T}(x) = \begin{bmatrix} \varphi(x) \\ L_f\varphi(x) \\ \vdots \\ L_f^{n-1}\varphi(x) \end{bmatrix}, \quad u(t) = \frac{{}^n\varphi(x)}{-L_g L_f^{n-1}\varphi(x)} + \frac{v(t)}{L_g L_f^{n-1}\varphi(x)} \quad (3.9)$$

the flat output then is

$$\lambda(x) = \varphi(x). \quad (3.10)$$

3.3 Feedback linearization for MIMO systems

The feedback linearization method can be extended to multiple input multiple output nonlinear systems [Sas99]. Let the MIMO nonlinear system have n states and m inputs/outputs where $x \in R^n$ is the state, $u \in R^m$ is the control input vector and $y \in R^m$ is the output vector. Similar to the SISO case, a vector relative degree is defined for the MIMO system in (3.1). The problem of finding the vector relative degree implies differentiation of each output signal until at least one of the input signals appears explicitly in the differentiation. For each output signal, we define r_j as the smallest integer such that at least one of the inputs appears in $y_j^{r_j}$:

$$y_j^{r_j} = L_f^{r_j} h_j + \sum_{i=1}^{m} L_{g_i}(L_f^{r_j-1} h_j)u_i. \quad (3.11)$$

That is, for at least one term $L_{g_i}(L_f^{r_j-1} h_j)u_i = 0$ around x. In what follows we assume that the sum of the relative degrees of each output is equal to the number of states of the nonlinear system. Such an assumption implies that the feedback linearization method is exact. Thus, neither of the state variables of the original nonlinear system is rendered unobservable through feedback linearization. The matrix $\mathbf{M}(x)$, defined as the decoupling matrix of the system, is given as:

$$\mathbf{M}(x) = \begin{bmatrix} L_{g_1} L_f^{r_1-1} h_1 & \cdots & L_{g_m} L_f^{r_1-1} h_1 \\ \vdots & \ddots & \vdots \\ L_{g_1} L_f^{r_m-1} h_m & \cdots & L_{g_m} L_f^{r_m-1} h_m \end{bmatrix}. \quad (3.12)$$

The nonlinear system in (3.1) has a defined vector relative degree $(r_1, r_2, \ldots, r_m)$ at the point x_0 if $L_{g_i} L_f^k h_i(x_0) = 0$ for $0 \le k \le r_i - 2$ and $i = 1, \ldots, m$ and given that

the matrix $\mathbf{M}(x_0)$ is nonsingular. If the vector relative degree $(r_1, r_2, \ldots, r_m)$ is well defined then (3.11) can be written as

$$
\begin{bmatrix} y_1^{r_1} \\ y_2^{r_2} \\ \vdots \\ y_m^{r_m} \end{bmatrix} = \begin{bmatrix} L_f^{r_1} h_1 \\ L_f^{r_2} h_2 \\ \vdots \\ L_f^{r_m} h_m \end{bmatrix} + \mathbf{M}(x) \begin{bmatrix} u_1 \\ u_2 \\ \vdots \\ u_m \end{bmatrix}
\tag{3.13}
$$

and since $\mathbf{M}(x_0)$ is nonsingular then also $\mathbf{M}(x) \in \mathsf{R}^{m \times m}$ is nonsingular in a neighborhood x of x_0. As a consequence, the control vector may be chosen as

$$
\begin{bmatrix} u_1 \\ u_2 \\ \vdots \\ u_m \end{bmatrix} = -\mathbf{M}^{-1}(x) \begin{bmatrix} L_f^{r_1} h_1 \\ L_f^{r_2} h_2 \\ \vdots \\ L_f^{r_m} h_m \end{bmatrix} + \mathbf{M}^{-1}(x) \begin{bmatrix} y_1^{r_1} \\ y_2^{r_2} \\ \vdots \\ y_m^{r_m} \end{bmatrix}
\tag{3.14}
$$

that is

$$
u = \rho(x) + \gamma(x)v
\tag{3.15}
$$

where

$$
\gamma(x) = -\mathbf{M}^{-1}(x), \ u = \begin{bmatrix} u_1 \\ u_2 \\ \vdots \\ u_m \end{bmatrix}, \ v = \begin{bmatrix} y_1^{r_1} \\ y_2^{r_2} \\ \vdots \\ y_m^{r_m} \end{bmatrix}, \ \rho(x) = -\mathbf{M}^{-1}(x) \begin{bmatrix} L_f^{r_1} h_1 \\ L_f^{r_2} h_2 \\ \vdots \\ L_f^{r_m} h_m \end{bmatrix}
$$

Letting the states x undergo the change of coordinates

$$
x_z = \begin{bmatrix} y_1 & \cdots & L_f^{r_1-1} y_1 & y_2 & \cdots & L_f^{r_2-1} y_2 & \cdots & \cdots & y_m & \cdots & L_f^{r_m-1} y_m \end{bmatrix}^{\mathsf{T}}
\tag{3.16}
$$

the nonlinear MIMO system in (3.1) is linearized, yielding

$$
\dot{x}_z = \mathbf{A}_z x_z + \mathbf{B}_z v
\tag{3.17}
$$

with

$$
\mathbf{A}_z = \mathrm{diag}(\mathbf{A}_{z_1} \ldots \mathbf{A}_{z_m}) \quad \mathbf{B}_z = \mathrm{diag}(\mathbf{B}_{z_1} \ldots \mathbf{B}_{z_m}),
\tag{3.18}
$$

where each term individually is given by:

$$\mathbf{A}_{z_i} = \begin{bmatrix} 0 & 1 & 0 & \dots & 0 \\ 0 & 0 & 1 & \dots & 0 \\ & \ddots & \ddots & \ddots & \\ 0 & 0 & 0 & \dots & 1 \\ & & & & \\ 0 & 0 & 0 & \dots & 0 \end{bmatrix}, \quad \mathbf{B}_{z_i} = \begin{bmatrix} 0 \\ 0 \\ 0 \\ \vdots \\ \vdots \\ 1 \end{bmatrix}$$

By a feedback control law and a state transformation, the feedback linearization is acquired, resulting in a linearized system in the form of a chain of integrators [Isi95]. The design of the linear controller is easy, however, the interpretation is complicated because the linearized system obtained does not have a physical meaning similar to the initial nonlinear system. Indeed, two nonlinear systems having the same vector relative degree will result in the same feedback linearized system.

3.4 Flat Output

Due to the definition of the trolley acceleration and cable extension acceleration as inputs $u = [\ddot{x}_c(t)\ \ddot{y}_c(t)\ \ddot{l}(t)] \in \mathbb{R}^3$ instead of the respective forces the two equations (2.12) are independent of the mass of the load. Therefore, the only parameter is the acceleration of gravity g. The trolley moves in the x and y directions and the rope are controlled by a lower-motor controller whose speeds can be commanded. The forces of the oscillating load on the car and the winch will be governed by these controllers, hence, a simple double-integrating behavior is may be considered as the possible reactions of the load which could not be compensated as disturbances. Thus, with

$$u = \begin{bmatrix} u_x & \dot{u}_y & u_l \end{bmatrix}^T \tag{3.19}$$

and substituting

$$\ddot{x}_c = u_x, \quad \ddot{y}_c = u_y, \quad \ddot{l} = u_l. \tag{3.20}$$

into (2.12) we arrive at the state vector

$$x = \begin{bmatrix} x_c & \dot{x}_c & y_c & \dot{y}_c & l & \dot{l} & \alpha & \dot{\alpha} & \beta & \dot{\beta} \end{bmatrix}^T \in \mathbb{R}^{10} \tag{3.21}$$

with respect to the following equivalent nonlinear system

$$\dot{x} = f(x) + g(x)u \quad , \quad x(0) = x_0. \tag{3.22}$$

In the next steps, it s shown that the dynamic model of the gantry crane is differentially flat with the position of the load as flat output. In terms of the flat output it is possble to paramterize both the states and inputs of the system as per

$$x = \phi_x(z, \dot{z}, \ldots, z^{(n-1)}) \tag{3.23a}$$

$$u = \phi_u(z, \dot{z}, \ldots, z^{(n)}). \tag{3.23b}$$

With this property the system allows for an exact input/state linearization of the complete crane dynamics and simplifies these to three integrator chains, appropriately. The subsequent control design is well simplified using linear methods again. The position of the load as the output z of the system yields

$$z = \begin{bmatrix} z_1 \\ z_2 \\ z_3 \end{bmatrix} = h(x) = r_l(t) = \begin{bmatrix} x_c(t) + l(t)\sin(\beta) \\ y_c(t) + l(t)\cos(\beta)\sin(\alpha) \\ -l(t)\cos(\alpha)\cos(\beta). \end{bmatrix}. \tag{3.24}$$

Calculating the first derivative of the output results in

$$\dot{z} = L_f h(x) + L_g h(x) u = L_f h(x)$$
$$= \begin{bmatrix} \dot{x}_c + \dot{l}\sin(\beta) + l\dot{\beta}\cos(\beta) \\ \dot{y}_c + \dot{l}\cos(\beta)\sin(\alpha) + l\dot{\alpha}\cos(\alpha)\cos(\beta) - l\dot{\beta}\sin(\alpha)\sin(\beta) \\ -\dot{l}\cos(\alpha)\cos(\beta) + l\dot{\alpha}\cos(\beta)\sin(\alpha) + l\dot{\beta}\cos(\alpha)\sin(\beta) \end{bmatrix} \tag{3.25}$$

The acceleration of load is obtained by differentiating again,

$$\ddot{z} = L_f^2 h(x) + L_g L_f h(x) u = \begin{bmatrix} \sin(\beta) \\ \cos(\beta)\sin(\alpha) \\ -\cos(\alpha)\cos(\beta) \end{bmatrix} a_r(x, u) - \begin{bmatrix} 0 \\ 0 \\ g \end{bmatrix} \tag{3.26}$$

where

$$a_r(x, u) = \ddot{x}_c\sin(\beta) + \ddot{y}_c\sin(\alpha)\cos(\beta) + \ddot{l} - g\cos(\alpha)\cos(\beta) - l\dot{\alpha}^2\cos^2(\beta) - l\dot{\beta}^2. \tag{3.27}$$

Based on [KKS10] the equation (3.27) represent the acceleration generated by the rope force $a_r(x, u) = q_r/m$.

Thus, equation (3.26) can be expressed as follows:

$$\ddot{z} = \begin{bmatrix} a_r \sin(\beta) \\ a_r \cos(\beta) \sin(\alpha) \\ -g - a_r \cos(\alpha) \cos(\beta) \end{bmatrix}. \tag{3.28}$$

Equation (3.28) express the consequence of the principle of linear momentum of the load

$$\bar{l}_r = \bar{Q} q_r \tag{3.29}$$

$$\bar{Q} = \frac{r_t(t) - r_l(t)}{||r_t(t) - r_l(t)||} = \begin{bmatrix} \sin(\beta) \\ \cos(\beta) \sin(\alpha) \\ -\cos(\alpha) \cos(\beta) \end{bmatrix}. \tag{3.30}$$

Now we proceed to derive (3.28) with respect to time again, yielding the third and fourth derivative of the load position

$$\overset{(3)}{z} = \begin{bmatrix} a_r \dot{\beta} \cos(\beta) + \dot{a}_r \sin(\beta) \\ -a_r \dot{\beta} \sin(\alpha) \sin(\beta) + a_r \dot{\alpha} \cos(\beta) \cos(\alpha) + \dot{a}_r \cos(\beta) \sin(\alpha) \\ a_r \dot{\beta} \sin(\beta) \cos(\alpha) + a_r \dot{\alpha} \cos(\beta) \sin(\alpha) - \dot{a}_r \cos(\beta) \cos(\alpha) \end{bmatrix}, \tag{3.31}$$

$$\overset{(4)}{z} = \begin{bmatrix} \overset{(4)}{z}_1(x, u, a_r, \dot{a}_r, \ddot{a}_r) \\ \overset{(4)}{z}_2(x, u, a_r, \dot{a}_r, \ddot{a}_r) \\ \overset{(4)}{z}_3(x, u, a_r, \dot{a}_r, \ddot{a}_r) \end{bmatrix}. \tag{3.32}$$

The utility of the expression $a_r(x, u)$ will be explained further in the next sections.

3.5 Parametrization of the States

After that we have derived the dependence on the load position, velocity and further derivatives with respect to the states x, the inputs u and the acceleration alongside the rope a_r, we now have a second parametrization of the states x and inputs u with respect to the position of the load z.

For evaluating the cardan angles α and β we use the acceleration $\ddot{z}$ in (3.28). Projection of (3.28) onto a line which is orthogonal to the rope as well as to the x, respectively

the *y*-axis, allows us to eliminate the unknown acceleration a_r such that

$$\ddot{z}_2 \cos(\alpha) + \ddot{z}_3 \sin(\alpha) = -g \sin(\alpha) \tag{3.33}$$

which can be solved for α, that is

$$\alpha = \phi_{x_7} = -\arctan\left[\frac{\ddot{z}_2}{\ddot{z}_3 + g}\right]. \tag{3.34}$$

Projecting (3.28) onto the line orthogonal to the *y*-axis yields

$$\ddot{z}_3 \sin(\beta) + \ddot{z}_1 \cos(\beta) \cos(\alpha) = -g \sin(\beta) \tag{3.35}$$

which can be solved for β, hence

$$\beta = \phi_{x_9} = -\arctan\left[\frac{\ddot{z}_1 \cos(\alpha)}{\ddot{z}_3 + g}\right]. \tag{3.36}$$

Furthermore (3.24) can be solved for x_c, y_c and l which results in

$$l = {}^x\phi = \frac{z_3}{\cos(\beta) \cos(\alpha)} \tag{3.37a}$$

$$y_c = \phi_{x_3} = -l \cos(\beta) \sin(\alpha) + z_2 \tag{3.37b}$$

$$x_c = \phi_{x_1} = -l \sin(\beta) + z_1. \tag{3.37c}$$

By derivation of (3.34) and (3.36) we obtain the parameterizations for cardan angle velocities $\dot{\alpha}$, $\dot{\beta}$ and by derivation (3.37), we yield the trolley velocities $\dot{x}_c$ and $\dot{y}_c$ as well as the rope speed $\dot{l}$

$$\frac{d}{dt}\left[\phi^{x_1}\ \phi_{x_3}\ \phi_{x_5}\ \phi_{x_7}\ \phi_{x_9}\right]^{\cdot T} = \left[\dot{\phi}_{x_2}\ \dot{\phi}_{x_4}\ \phi_{x_6}\ \phi_{x_8}\ \phi_{x_{10}}\right]^{\cdot T}. \tag{3.38}$$

The parameterization of the input vector *u* can be found by solving the second derivative of (3.37).

$$u_x = \dddot{x}_c = \phi_{u_x}(z, \dot{z}, \ddot{z}, \overset{(3)}{z}, \overset{(4)}{z}) \tag{3.39a}$$

$$u_y = \dddot{y}_c = \phi_{u_y}(z, \dot{z}, \ddot{z}, \overset{(3)}{z}, \overset{(4)}{z}) \tag{3.39b}$$

$$u_l = \ddot{l} = \phi_{u_l}(z, \dot{z}, \ddot{z}, \overset{(3)}{z}, \overset{(4)}{z}). \tag{3.39c}$$

This results in a parameterization of the states *x* as well as the inputs *u* with respect to the position of the load *z* and its time derivatives. Therefore the system derived here is flat, where the position of the load is a flat output of the system.

3.6 Exact Input/Output Linearization

The system in Section 2 with the parameterization given in Section 3.5 is flat. The system present ten states (3.21), therefore, the sum of the vectorial relative degree *r* has to be ten as well. Hence we have *r* = [4 4 2]. Using (3.24) we can compute the measured load positions z_m by measurements of the states *x*, the same is possible for the load velocities $\dot{z}_m$ by (3.25). In this case, the second derivative $\ddot{z}$ of the load still depends on the full input *u*. By application of the results obtained in (3.28) related to linear momentum and the acceleration along the rope $a_r(x, u)$, the expression is as follows [KKS10],

$$\ddot{z} = L_f^2 h(x) + L_g L_f h(x) u = \ddot{z}_m = \begin{bmatrix} \ddot{z}_{1,m} \\ \ddot{z}_{2,m} \\ \ddot{z}_{3,m} \end{bmatrix} = \begin{bmatrix} \Phi_{\ddot{z}_{1,m}}(x, u) \\ \Phi_{\ddot{z}_{2,m}}(x, u) \\ \Phi_{\ddot{z}_{3,m}}(x, u) \end{bmatrix} = \begin{bmatrix} a_r \sin(\beta) \\ a_r \, \cos(\beta) \, \sin(\alpha) \\ -g - a_r \cos(\alpha) \cos(\beta) \end{bmatrix}.$$

$$(3.40)$$

Assuming the relative degree of z_3 to be two, the second derivative of z_3 is equal to the new virtual input v_3, that is

$$\ddot{z}_{3,m} = -g - \cos(\beta) \cos(\alpha) a_r = v_3, \tag{3.41}$$

which can be solved for a_r to yield

$$a_r = -\frac{v_3 + g}{\cos(\beta) \, \cos(\alpha)} \tag{3.42}$$

Replacement of a_r in (3.40) yields $\ddot{z}_{1,m}$ and $\ddot{z}_{2,m}$, $\ddot{z}_{3,m}$, known from (3.41)

$$\ddot{z}_{1,m} = -\sin(\beta) \frac{v_3 + g}{\cos(\beta)\cos(\alpha)} \tag{3.43a}$$

$$\ddot{z}_{2,m} = -\sin(\alpha) \frac{v_3 + g}{\cos(\alpha)} \tag{3.43b}$$

$$\ddot{z}_{3,m} = v_3, \tag{3.43c}$$

and in the same way for the third derivative

$$\overset{(3)}{z}_1 = \Phi_{\overset{(3)}{z_1}}(x, v_3, \dot{v}_3) \tag{3.44a}$$

$$\overset{(3)}{z}_2 = \Phi_{\overset{(3)}{z_2}}(x, v_3, \dot{v}_3) \tag{3.44b}$$

$$\overset{(3)}{z}_3 = \dot{v}_3, \tag{3.44c}$$

as well as the forth derivative

$$\overset{(4)}{z}_1 = \Phi_{\overset{(4)}{z_1}}(x, u, v_3, \dot{v}_3, \ddot{v}_3) \tag{3.45a}$$

$$\overset{(4)}{z}_2 = \Phi_{\overset{(4)}{z_2}}(x, u, v_3, \dot{v}_3, \ddot{v}_3) \tag{3.45b}$$

$$\overset{(4)}{z}_3 = \ddot{v}_3. \tag{3.45c}$$

The previous equations show that the fourth derivative of $z_{1,m}$ and $z_{2,m}$ is once again depending on the input vector u. Taking into account the relative degree and replacing the derivatives of z_3 by the adequate derivatives of v_3 we present three equations containing the inputs u_x, u_y and u_l of the system:

$$v_1 = \Phi_{\overset{(4)}{z_1}}(x, u, v_3, \dot{v}_3, \ddot{v}_3) \tag{3.46a}$$

$$v_2 = \Phi_{\overset{(4)}{z_2}}(x, u, v_3, \dot{v}_3, \ddot{v}_3) \tag{3.46b}$$

$$v_3 = \Phi_{\ddot{z}_3}(x, u) \tag{3.46c}$$

where v_1 and v_2 are the virtual inputs to the forth derivative of z_1 and z_2. For achieving trajectory tracking control we set all three components independently from each other. Therefore, the non-linear system of equations may be solved for the three inputs $u = [u_x \ u_y \ u_l]$. The dynamic system (3.45) is in Brunovský normal form and consists of three integrator chains of length 4. For the reactions of the control action, the error variables $e_z = [e_{z_1} \ e_{z_2} \ e_{z_3}]^T = (z_d - z)$ are introduced. The two virtual inputs v_1, v_2 and the second derivative of the third virtual input $\ddot{v}_3$ are chosen as follows

$$v_1 = \overset{(4)}{z}_{1,d} + k_{1,0}e_{z_1} + k_{1,1}\dot{e}_{z_1} + k_{1,2}\ddot{e}_{z_1} + k_{1,3}\overset{(3)}{e}_{z_1} \tag{3.47a}$$

$$v_2 = \overset{(4)}{z}_{2,d} + k_{2,0}e_{z_2} + k_{2,1}\dot{e}_{z_2} + k_{2,2}\ddot{e}_{z_2} + k_{2,3}\overset{(3)}{e}_{z_2} \tag{3.47b}$$

$$\ddot{v}_3 = \overset{(4)}{z}_{3,d} + k_{3,0}e_{z_3} + k_{3,1}\dot{e}_{z_3} + k_{3,2}\ddot{e}_{z_3} + k_{3,3}\overset{(3)}{e}_{z_3} \tag{3.47c}$$

where $k_{1,0...3}$, $k_{2,0...3}$ and $k_{3,0...3}$ are selected each to match with a a Hurwitz polynomial in order to achieve a stable tracking behavior. The reference trajectory z_d must be chosen four times differentiable in all three components, that is $z_d \in C^4$. It is important to note that by equation (3.47c) the system dynamics of the third component of the flat output is a double integrator which is extended and implemented in the controller. This results in a dynamic controller. Figure 3.1 shows the structure of the control loop, indictaing the main signal flows.
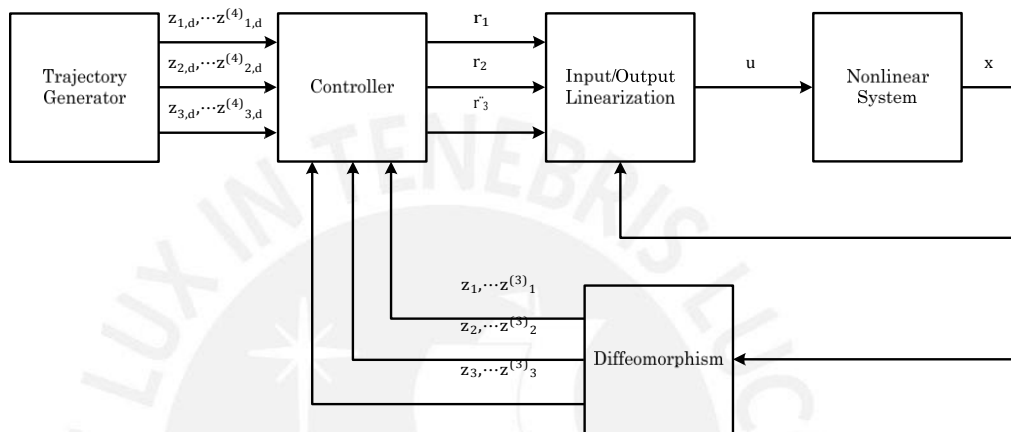
Figure 3.1: Signal flow diagram of the derived tracking controller.

4 Tracking Controller Design

4.1 Trajectory generation

In this part we will focus on the method used to calculate a trajectory that describes the desired crane movement in the multidimensional space. For more details see [Cra14] and [Bar12]. Here, path refers to a record at the time of the position, velocity and acceleration for each degree of freedom.

This includes the problem of specifying a suitable path or route through the workspace. To facilitate the description of motion of the system, depending on the requirements, functions of position and time will be chosen to specify the task. Then, the equation which represent descriptions of the desired movement are taken on the basis of theory presented above. In this case, the desired load position is indicated and according to the description for the generation of the propagation path the desired goal is reached. This then includes the length, the velocity profile and other details.

Consider the problem of moving the load from its initial position to a target position within a certain amount of time. Inverse kinematics may be used to calculate the set of joint angles corresponding to the position and orientation target. The initial position of the system is known in the form of a set of joint angles and displacements. Then, a function is required for each joint, whose value at time t_0 is the initial position of the joint and whose value at time t_f is the desired position of the joint at a final time instant.

To create a single move at least four boundary conditions on the function $\theta = \theta(t)$ are required. Two of these restrictions on the value of the function are due to the selection of initial and final values, that is

$$
\begin{aligned}
\theta(0) &= \theta_0, \\
\theta(t_f) &= \theta_f.
\end{aligned}
\tag{4.1}
$$

The other two restrictions are that the function must be stationary at t_0 and t_f. This

means that the initial and final velocities must be zero, hence

$$\dot{\theta}(0) = 0,$$
$$\dot{\theta}(t_f) = 0. \tag{4.2}$$

These four constraints can be satisfied by a polynomial of at least third degree. In the situation that the output conditions require a higher order of differentiability at the nitial and final point, as in this case, higher degree polynomials for path segments are used. Then, if we specify the position, velocity and acceleration at the beginning and end of each route segment a fifth degree polynomial is required, say

$$\theta(t) = a_0 + a_1 t + a_2 t^2 + a_3 t^3 + a_4 t^4 + a_5 t^5, \tag{4.3}$$

where the restrictions are given as follows

$$\theta_0 = a_0,$$
$$\theta_f = a_0 + a_1 t_f + a_2 t_f^2 + a_3 t_f^3 + a_4 t_f^4 + a_5 t_f^5,$$
$$\dot{\theta}_0 = a_1,$$
$$\dot{\theta}_f = a_1 + 2a_2 t_f + 3a_3 t_f^2 + 4a_4 t_f^3 + 5a_5 t_f^4,$$
$$\ddot{\theta}_0 = 2a_2,$$
$$\ddot{\theta}_f = 2a_2 + 6a_3 t_f + 12a_4 t_f^2 + 20a_5 t_f^3. \tag{4.4}$$

These constraints yield a set of six linear equations in six unknowns whose solution are

$$a_0 = \theta_0,$$
$$a_1 = \dot{\theta}_0,$$
$$a_2 = \frac{\ddot{\theta}_0}{2},$$
$$a_3 = \frac{20\theta_f - 20\theta_0 - (8\dot{\theta}_f + 12\dot{\theta}_0)t_f - (3\ddot{\theta}_0 - \ddot{\theta}_f)t_f^2}{2t_f^3},$$
$$a_4 = \frac{30\theta_0 - 30\theta_f + (14\dot{\theta}_f + 16\dot{\theta}_0)t_f + (3\ddot{\theta}_0 - 2\ddot{\theta}_f)t_f^2}{2t_f^4},$$
$$a_5 = \frac{12\theta_f - 12\theta_0 - (6\dot{\theta}_f + 6\dot{\theta}_0)t_f - (\ddot{\theta}_0 - \ddot{\theta}_f)t_f^2}{2t_f^5}. \tag{4.5}$$

Figure 4.1 shows the response of the trajectory in position, speed, and acceleration according to (4.3). We notice that the acceleration vanishes in t_0 and t_f.

(a) Position $\theta(t)$ (b) Speed $\dot{\theta}(t)$ (c) Acceleration $\ddot{\theta}(t)$
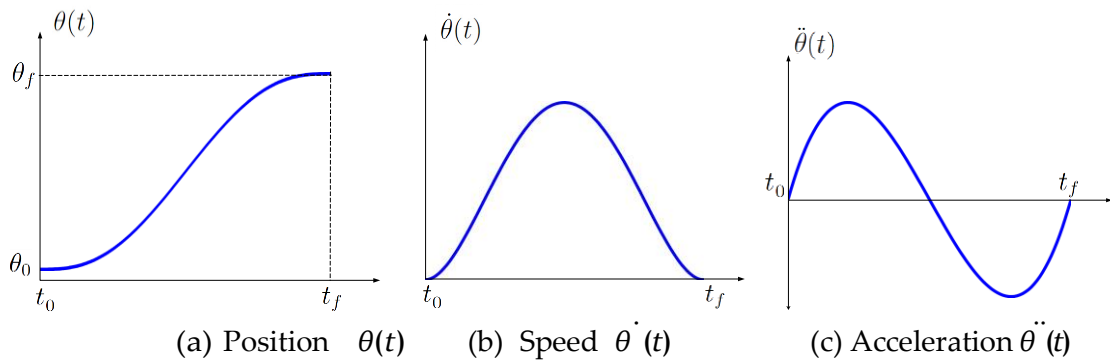
Figure 4.1: Trajectory generation response.

4.2 Linearized System Control

With the result obtained in the previous chapters we are now able to obtain a feedback-equivalent linear system, based in the nonlinear equation (3.22). Note that the states are made up by the control error shown in (3.47). Figure 4.2 presents a block diagram of the linearized system.
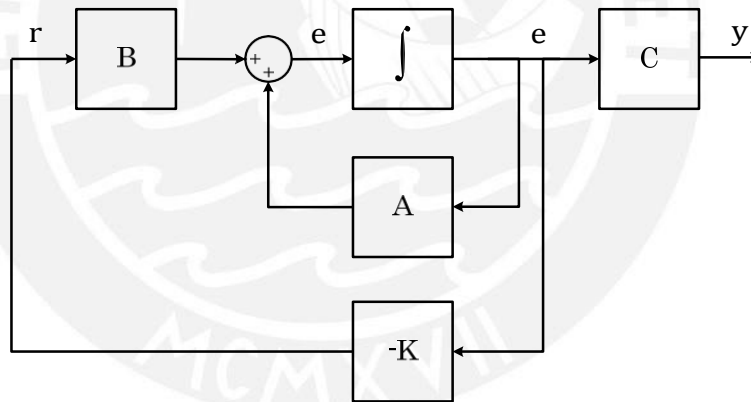
Figure 4.2: Closed-loop control system with $v = -\mathbf{K}e$.

The system has the following state space equation

$$\dot{e} = \mathbf{A}e + \mathbf{B}v \ , \ y = \mathbf{C}e \tag{4.6}$$

where

$$\mathbf{A} = \begin{bmatrix} 0 & 1 & 0 & 0 & 0 & 0 & 0 & 0 & 0 & 0 & 0 \\ 0 & 0 & 1 & 0 & 0 & 0 & 0 & 0 & 0 & 0 & 0 \\ 0 & 0 & 0 & 1 & 0 & 0 & 0 & 0 & 0 & 0 & 0 \\ 0 & 0 & 0 & 0 & 0 & 0 & 0 & 0 & 0 & 0 & 0 \\ 0 & 0 & 0 & 0 & 0 & 1 & 0 & 0 & 0 & 0 & 0 \\ 0 & 0 & 0 & 0 & 0 & 0 & 1 & 0 & 0 & 0 & 0 \\ 0 & 0 & 0 & 0 & 0 & 0 & 0 & 1 & 0 & 0 & 0 \\ 0 & 0 & 0 & 0 & 0 & 0 & 0 & 0 & 0 & 0 & 0 \\ 0 & 0 & 0 & 0 & 0 & 0 & 0 & 0 & 0 & 1 & 0 \\ 0 & 0 & 0 & 0 & 0 & 0 & 0 & 0 & 0 & 0 & 1 \\ 0 & 0 & 0 & 0 & 0 & 0 & 0 & 0 & 0 & 0 & 0 \\ 0 & 0 & 0 & 0 & 0 & 0 & 0 & 0 & 0 & 0 & 0 \end{bmatrix}, \quad \mathbf{B} = \begin{bmatrix} 0 & 0 & 0 \\ 0 & 0 & 0 \\ 0 & 0 & 0 \\ 1 & 0 & 0 \\ 0 & 0 & 0 \\ 0 & 0 & 0 \\ 0 & 0 & 0 \\ 0 & 1 & 0 \\ 0 & 0 & 0 \\ 0 & 0 & 0 \\ 0 & 0 & 0 \\ 0 & 0 & 1 \end{bmatrix} \tag{4.7}$$

$$\mathbf{C} = \begin{bmatrix} 1 & 0 & 0 & 0 & 0 & 0 & 0 & 0 & 0 & 0 & 0 \\ 0 & 0 & 0 & 0 & 1 & 0 & 0 & 0 & 0 & 0 & 0 \\ 0 & 0 & 0 & 0 & 0 & 0 & 0 & 1 & 0 & 0 & 0 \end{bmatrix} \tag{4.8}$$

Therefore, the main purpose in this chapter is to find the controller that achieve both translation of the payload and robust in presence of perturbations.

4.2.1 Pole Placement Control

Contrary to the conventional design only specifying dominant closed-loop poles, the pole placement approach specifies all closed-loop poles, given the condition that the system is completely state controllable [Oga10].

Based on system (4.6) we shall choose the control signal to be

$$v = -\mathbf{K}e. \tag{4.9}$$

The control signal v in this case is determined by a static state feedback. The matrix $\mathbf{K}$ is called the gain matrix. We need to guarantee that all state variables are available for feedback. The input v in this case is unconstrained. Recall that Figure 4.2 shows the structure of this system.

Substituting (4.9) into (4.6) gives

$$\dot{e}(t) = (\mathbf{A} - \mathbf{B}\mathbf{K})e(t) \tag{4.10}$$

whose initial value problem has the solution

$$e(t) = s^{(\mathbf{A}-\mathbf{BK})}e(0). \tag{4.11}$$

In this case, $e(0)$ is the unkown initial state. The stability of the system is determinated by the real part of eigenvalues wrt. matrix $\mathbf{A} - \mathbf{BK}$. Given that the system is controllable, the gain matrix $\mathbf{K}$ can be chosen such the error dynamics is asymptotically stable. In our case, the direct substitution method is used. Taking advantage of the symmetry regarding the x and y axes of the system we choose one of the equations, for example

$$v_1 = \overset{(4)}{z}_{1,d} + k_{1,0}e_{z_1} + k_{1,1}\dot{e}_{z_1} + k_{1,2}\ddot{e}_{z_1} + k_{1,3}\overset{(3)}{e}_{z_1}. \tag{4.12}$$

The reduced forth order equation to be evaluated is then

$$\dot{e}_1 = \mathbf{A}_1 e_1 + \mathbf{B}_1 v_1. \tag{4.13}$$

We construct the desired characteristic polynomial selecting the desired poles μ_i, that is

$$|s\mathbf{I} - \mathbf{A} - \mathbf{BK}| = |s\mathbf{I} - \tilde{\mathbf{A}}| = (s - \mu_1)(s - \mu_2)\dots(s - \mu_n)$$

$$= s^n + \alpha_1 s^{n-1} + \cdots + \alpha_{n\_1}s + \alpha_n = 0$$

Both sides of this characteristic equation are polynomials in s, hence, by equating coefficients it is possible to determine the values of $\mathbf{K}$. Finally, we test the obtained values with the y axis and the rope displacement l expressed in the linear space state model. The results are explained in details in the next chapter.

4.2.2 Linear Quadratic Regulator

An advantage of the quadratic optimal control method over pole-placement is that the former provides a automated way of finding an appropriate state-feedback controller. We shall now consider the optimal regulator problem that, given the system equation

$$\dot{e} = \mathbf{A}e + \mathbf{B}v \tag{4.14}$$

determines the matrix $\mathbf{K}$ of the optimal controller

$$v = -\mathbf{K}e(t) \tag{4.15}$$

so as to minimize the performance index

$$J = \int_0^\infty (e^* \mathbf{Q} e + v^* \mathbf{R} v)\, dt \qquad (4.16)$$

where $\mathbf{Q}$ is a positive-definite (or positive-semidefinite) Hermitian or real symmetric matrix and $\mathbf{R}$ is a positive-definite Hermitian or real symmetric matrix. Note that the second term on the right-hand side of (4.16) accounts for the 'energy consumption' of the control signals. The matrices $\mathbf{Q}$ and $\mathbf{R}$ determine the relative importance of the error and the 'consumption of the associated energy'. In this problem we assume that the control vector $u(t)$ is unconstrained.

In MATLAB, the command that solves the continuous-time, linear, quadratic regulator problem and the associated algebraic Riccati equation is called lqr(A,B,Q,R). This command calculates the optimal feedback gain matrix $\mathbf{K}$. Therefore, the goal for finding $\mathbf{K}$ is to choose appropriate values of the matrices $\mathbf{Q}$ and $\mathbf{R}$.

4.3 Robustification

In order to apply a robustification control on this system, first, we extend the equation (4.9) obtaining a new signal input

$$v + \mathbf{K}e(t) = \bar{v}. \qquad (4.17)$$

The equivalent plant is shown in Figure 4.3. In this section we implement two types
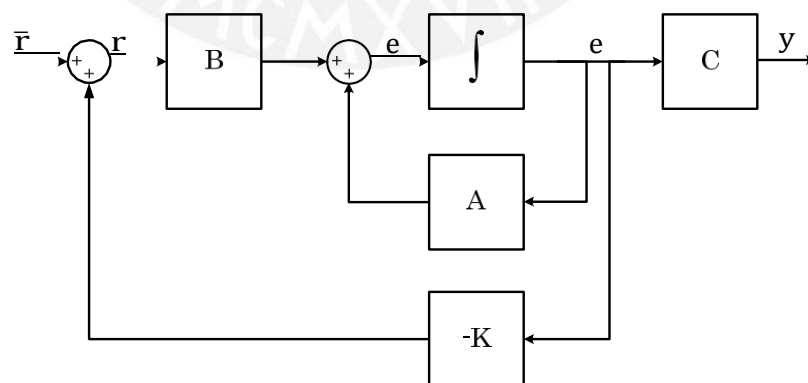
Figure 4.3: Space State System with Extension Input.

of robustification controls. Each will be tested to see the improvements in the output

control signal, especifically, in the attenuation of the disturbances.

4.3.1 H_∞ **Control**

First, some definitions and concepts are presented, which are needed in the design procedure. Let $\text{Re}(s)$ denote the real part of the complex number s and $\bar{\sigma}(M)$ the maximum singular value of matrix M.

Definition 1 (H_∞ - Space): The Space H_∞ is the Banach Space of matrix-valued complex functions $\mathbf{G}(s)$ declared on $j\text{R}$ which are analytic for $\text{Re}(s) > 0$ and bounded for $\text{Re}(s) = 0$. The H_∞-norm of G is defined as

$$||G||_\infty := \sup_{\omega \in \text{R}} \bar{\sigma}(G(j\omega)). \tag{4.18}$$

Definition 2 (RH_∞ - Space): The Space RH_∞ is the subspace of H_∞ of all real-stable rational, proper and stable transfer functions $G(s)$.

Let $RH_\infty^{p\times q}$ denote this space where the matrix transfer functions have dimension $p \times q$.

H_∞ - Standard Problem: In the H_∞ framework consider the generalized loop, shown in Figure 4.4. The inputs of the generalized system model $P(s)$ are build by internal inputs $u \in \text{R}^p$ (for example control variables) and the external inputs $w \in \text{R}^l$ (for example disturbanced). The outputs of the generalized system model consist of the internal outputs $v \in \text{R}^n$ (for example controlled output) and the external outputs $z \in \text{R}^m$.

This gives the input/output relation

$$\begin{bmatrix} z \\ v \end{bmatrix} = \underbrace{\begin{bmatrix} \mathbf{P}_{11} & \mathbf{P}_{12} \\ \mathbf{P}_{21} & \mathbf{P}_{22} \end{bmatrix}}_{\mathbf{P}(s)} \begin{bmatrix} w \\ u \end{bmatrix} . \tag{4.19}$$

The response of the external input $w \in \text{R}^l$ on the external outputs $z \in \text{R}^m$ can be easily determined as

$$\frac{Z(s)}{W(s)} = P_{11} + P_{12}K(I_{n\times n} - KP_{22})^{-1}P_{21} . \tag{4.20}$$

Based on the generalized plant model $P(s)$, the aim of the H_∞ design now is to find a stabilizing controller $K(s)$ that minimizes the H_∞-Norm of this transmission behavior and thus the maximum energy gain between external inputs and outputs. This menas
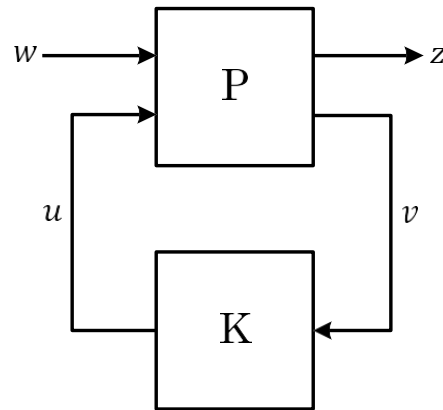
Figure 4.4: H_∞ Standard Problem

to solve

$$\inf_{K(s) \text{ stabilizing}} ||P_{11} + P_{12}K(I_{n \times n} - KP_{22})P_{21}||_\infty. \qquad (4.21)$$

For solving the H_∞ problem there are many ways. Most of them involve different configurations and weight functions to be minimized in the system [ZD98]. In this work, the model chosen is represented by the matrix (4.22) in a S/KS Mixed Sensitivity optimization. This configuration is used in systems for regulation problems. The block diagram is shown in Figure 4.5
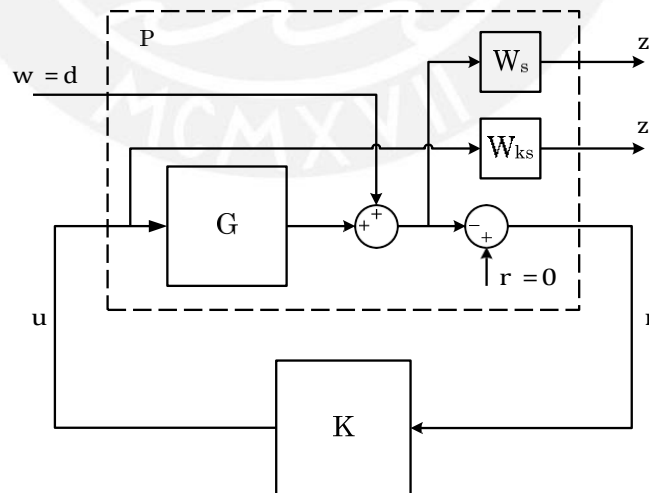
Figure 4.5: H_∞ S/KS Mixed Sensitivity Optimization in Standard Form (Regulation).

The corresponding input/output behavior reads

$$
\begin{bmatrix} z_1 \\ z_2 \\ v \end{bmatrix} = \begin{bmatrix} \mathbf{W}_s & \mathbf{W}_s \mathbf{G} \\ 0 & \mathbf{W}_{ks} \\ -\mathbf{I} & -\mathbf{G} \end{bmatrix} \begin{bmatrix} d \\ u \end{bmatrix} .
\tag{4.22}
$$

4.3.2 H_∞ Loop Shaping Control

A particular H_∞ loop-shaping design method is based on a Normalized Right Coprime Factorization of a transfer function.

Definition 4 (Normalized Right Coprime Factorization in RH_∞): The matrix pair $N(s) \in RH_\infty^{p \times q}$ and $M(s) \in RH_\infty^{p \times q}$ is called Normalized Right Coprime Factorization of a transfer matrix $G(s) \in RH_\infty^{p \times q}$, if

- $G(s) = N(s)M^{-1}(s)$,

- $M(s)$, $N(s)$ are right coprime in RH_∞,

- $M(s)M^T(-s) + N(s)N^T(-s) = I.$

To define quantitative criteria for the performance of the control loop, a desired profile of the singular values of the frequency response matrix of the open loop is specified. This shaping of the open loop (open loop shaping) is done by weighting the system model with suitable matrices $W_a(s)$ and $W_e(s)$, so that $G_s(s) = W_a(s)G(s)W_e(s)$. The corresponding H_∞ problem with the weighted system model $G(s)$ is then

$$
\inf_{K_w(s) \text{ stabilizing}} \left\| \begin{bmatrix} I_{p \times p} \\ K_w \end{bmatrix} (I_{p \times p} + G_w K_w)^{-1} M_w^{-1} \right\|_\infty = \frac{1}{\rho_{w,max}}.
\tag{4.23}
$$

Now given $K_w(s)$, the solution of the original control problem can be determined via $K(s) = W_a(s)K_w(s)W_e(s)$. The size $\rho_{w,max}$ can be regarded as a measure of the success of the design. This gained behaviour is depicted in Figure 4.6. Often, however, a stabilizing controller $K(s)$ which satisfies some of the quantitative requirements is previously known. Then the H_∞ loop-shaping design procedure, in this case, may yield a robustification of this controller. That means, a controller with similar quantitative characteristics is derived, but with increased robustness. For this purpose, only the open loop $G_w(s) = G(s)K(s)$ is given for the weighted distance model. The original weights arise accordingly to $W_a(s) = I_{p \times p}$ and $W_e(s) = K(s)$. The H_∞ loop-shaping design procedure is available in the MATLAB the function ncfsyn, as part of the Robust Control Toolboxes (based on the Glover-McFarlane Algorithm).
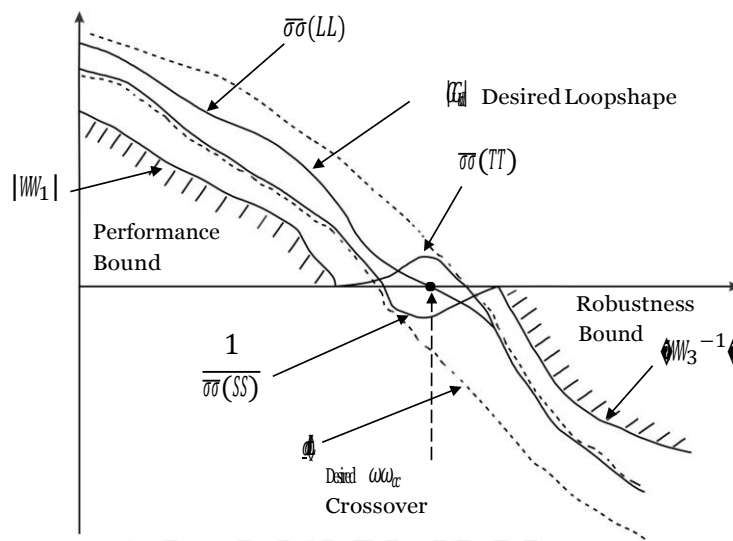
Figure 4.6: H_∞ Loop shaping Specifications.

The method of Glover-McFarlane Loop shaping consists of three steps [PD11]:

Step 1. Open loop shaping: Using a pre-weighting matrix W_e and an optional post-weighting matrix W_a, the minimum and maxiumum singular values are modified to shape the response. This step results in an augmented matrix of the process transfer function $G_s(s)$ shown in Figure 4.7.
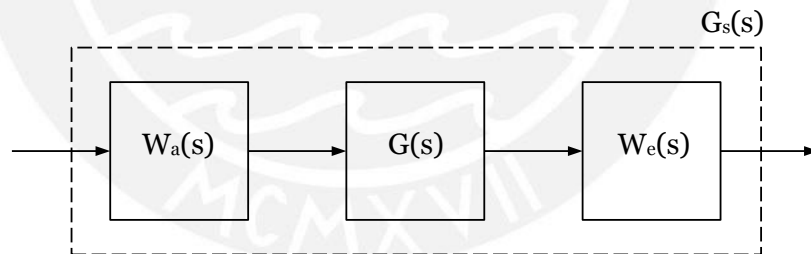
Figure 4.7: Augmented matrix of the process transfer function.

Step 2. Robust stability: The stability margin is computed as in (4.23). If $\rho_{w,max}$ 1 then the pre and post weighting matrices have to be modified by relaxing the constraints imposed on the open loop shape. If the value of $\rho_{w,max}$ is acceptable, for a value max $\rho < \rho_{w,max}$ the resulting controller K_w is computed in order to satisfy (4.23).

Step 3. Final robust controller: The final resulting controller is given by the sub-optimal controller K_w weighted with the matrices W_e or W_a obtaining as a result $K(s)$.
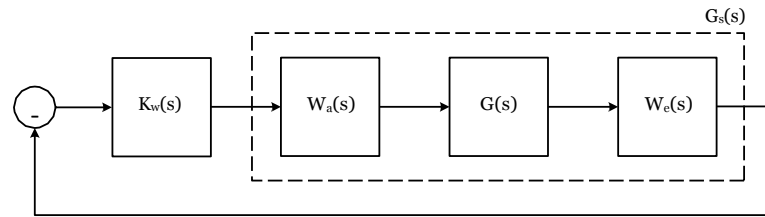
Figure 4.8: Robust closed loop control scheme.

Using the McFarlane-Glover method, the loop shaping is done without considering the problem of robust stability which is explcitily taken into account at the second design step by imposing a stability margin for the closed loop system. This stability margin $\rho_{w,max}$ is an indicator of the efficiency of the loop shaping technique.
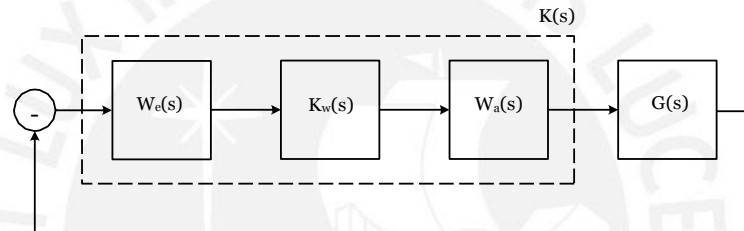
Figure 4.9: Optimal controller obtained with the pre and post weighting matrices.

5 Results of the Simulations

5.1 Simulink Blocks Simulation

All results of this work have been developed in MATLAB and its simulation tool SIMULINK. Figure 5.1 presents the shape of the simulation. Each part represents the process of linearization of the nonlinear system, starting with the nonlinear plant $\dot{x} = f(x) + g(x)u$ (Figure 5.2), the state transformation (diffeomorphism) and trajectory tracking (Figure 5.3) and the linearizing block $u = \phi(x) + \gamma(x)v$ (Figure 5.4). All these parts build the linearization block that we can see in Figure 5.5
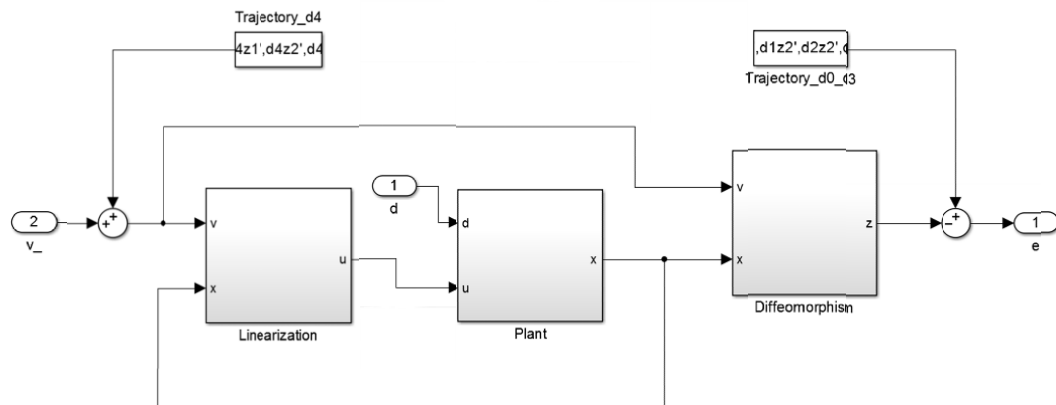
Figure 5.1: Simulink Model of the Linearized Plant.

Figure 5.5 presents the system extended and controlled by the state feedback controller. This block contains the parameters obtained via pole placement or LQR depending of the current analysis. In this figure, the block called Linearization represent the state space equation (4.6) where y is the new output of the linearized system.

In Figure 5.6, the system with robust controller is presented. The state space block is evaluated in both implementations, H_∞ and loop shaping robust control.
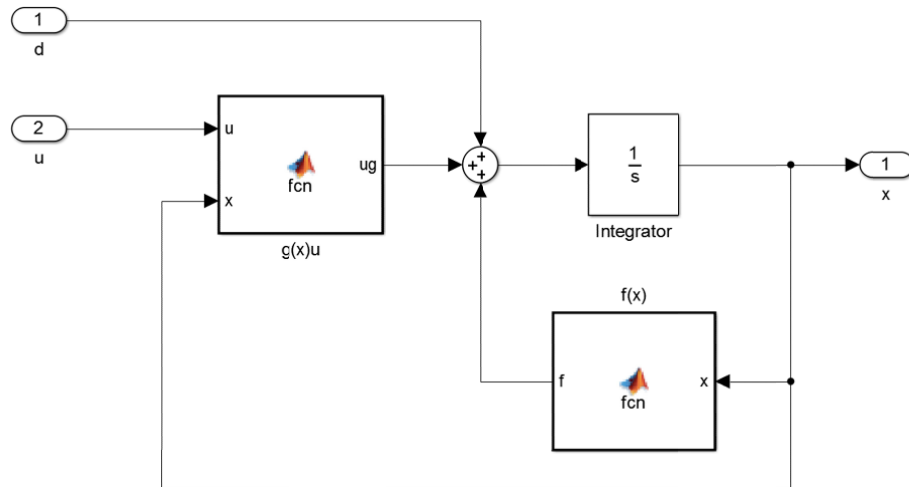
Figure 5.2: Nonlinear Plant $\dot{x} = f(x) + g(x)u$.
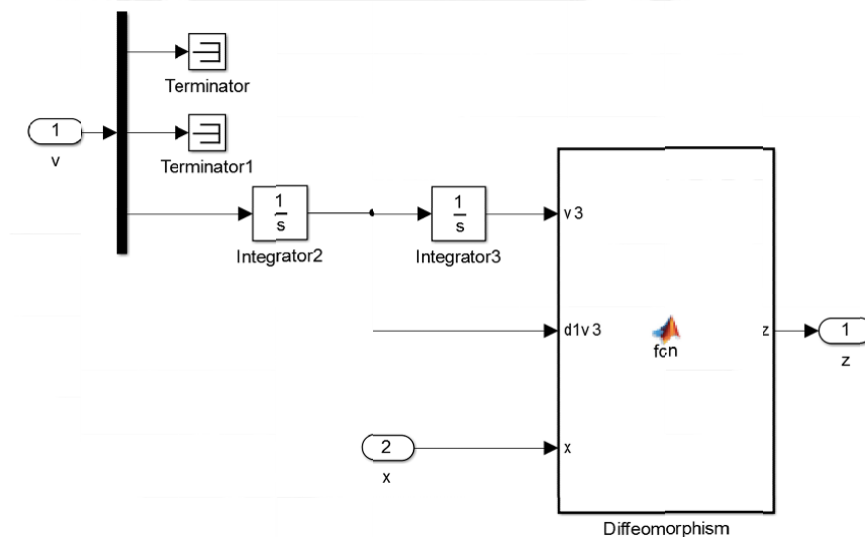
Figure 5.3: Diffeomorphism.

5.2 Control Response Tests

In this section, we explain the different procedures used for testing the system, both in control and robustification.

5.2.1 Control Values

The results of the evaluation of the linearized system for a Pole Placement control is based on the solution presented in (4.12) and (4.13). The feedback gains k, $z_{1|3}$ are
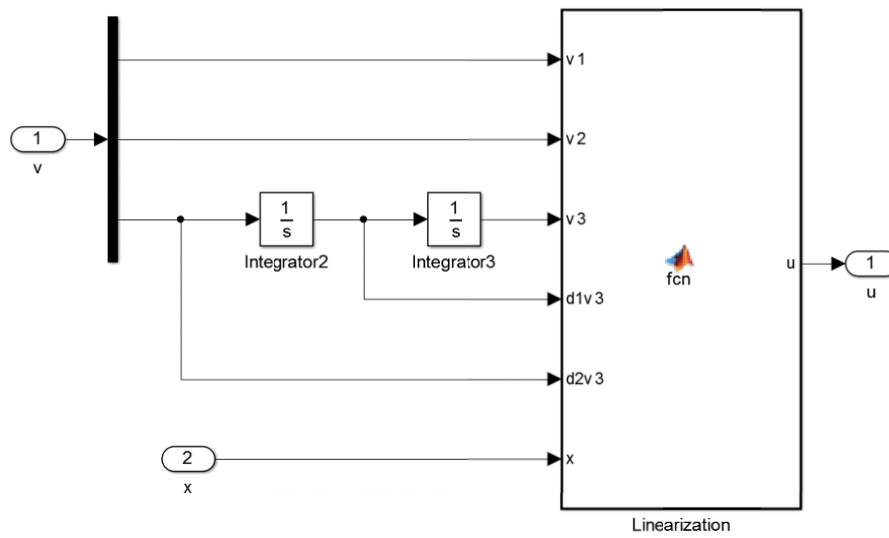
Figure 5.4: Linearization $u = \phi(x) + \gamma(x)v$.
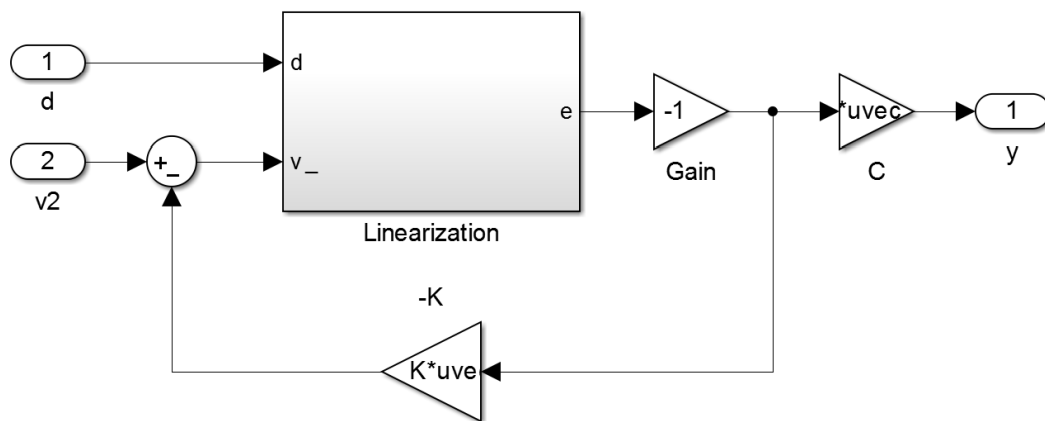
Figure 5.5: Linearization System with Extended Output $v + \mathbf{K}e(t) = \bar{v}$.

found by pole placement of the linear integrator chain of corresponding length. In this case we chose the poles at $\mu_{k,z_{1\,3}} = [-2.5 - 2.5 - 2.5 - 2.5]$.
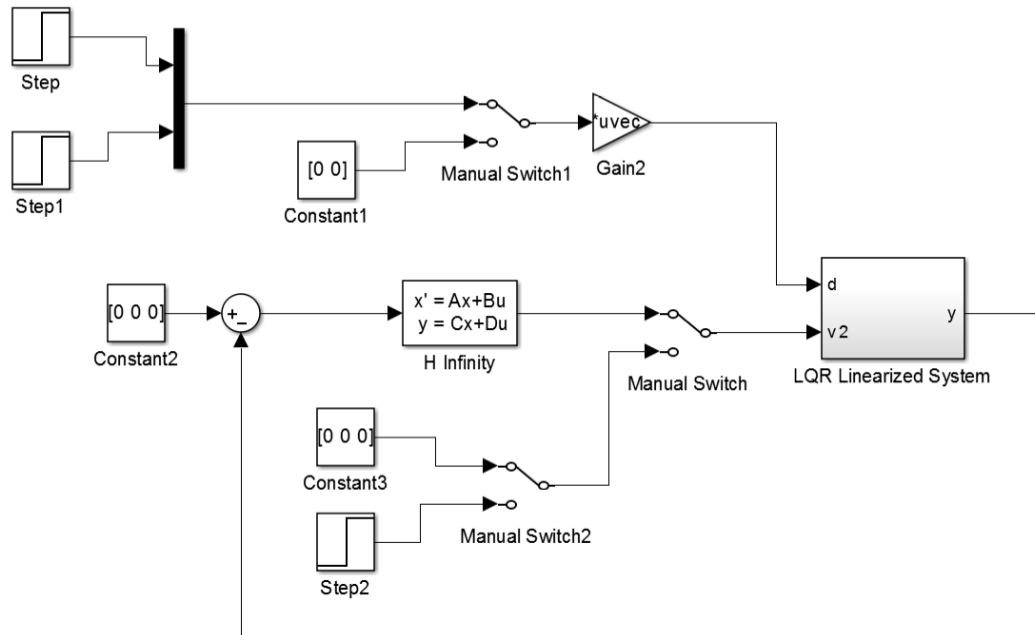
Figure 5.6: System with H_∞ Robustification.

With respect to the results obtained in LQR control, the matrixes **Q** and **R** are chosen in the following way:

$$
\mathbf{Q} = \begin{bmatrix}
1000 & 0 & 0 & 0 & 0 & 0 & 0 & 0 & 0 & 0 & 0 & 0 \\
0 & 1 & 0 & 0 & 0 & 0 & 0 & 0 & 0 & 0 & 0 & 0 \\
0 & 0 & 1 & 0 & 0 & 0 & 0 & 0 & 0 & 0 & 0 & 0 \\
0 & 0 & 0 & 1 & 0 & 0 & 0 & 0 & 0 & 0 & 0 & 0 \\
0 & 0 & 0 & 0 & 1000 & 0 & 0 & 0 & 0 & 0 & 0 & 0 \\
0 & 0 & 0 & 0 & 0 & 1 & 0 & 0 & 0 & 0 & 0 & 0 \\
0 & 0 & 0 & 0 & 0 & 0 & 1 & 0 & 0 & 0 & 0 & 0 \\
0 & 0 & 0 & 0 & 0 & 0 & 0 & 1 & 0 & 0 & 0 & 0 \\
0 & 0 & 0 & 0 & 0 & 0 & 0 & 0 & 1000 & 0 & 0 & 0 \\
0 & 0 & 0 & 0 & 0 & 0 & 0 & 0 & 0 & 1 & 0 & 0 \\
0 & 0 & 0 & 0 & 0 & 0 & 0 & 0 & 0 & 0 & 1 & 0 \\
0 & 0 & 0 & 0 & 0 & 0 & 0 & 0 & 0 & 0 & 0 & 1
\end{bmatrix}, \quad \mathbf{R} = \begin{bmatrix} 0.1 & 0 & 0 \\ 0 & 0.1 & 0 \\ 0 & 0 & 0.1 \end{bmatrix}
$$

These values are applied for the closed loop of the linearized system. The test of these values follows in the next sections.

Regarding the robustification of the system through H_∞ control, following the standard form S/KS mixed sensitivity approach presented in Section 4.3.1,   the selection of

the gains in $\mathbf{W}_s$ and $\mathbf{W}_{ks}$ are based on a Low Pass Filter and a low gain constant, respectively. The values of these gains require some iterations to obtain weights which will yield an acceptable controller. Respect to $\mathbf{W}_s$, the representation of the filter is the following:

$$\mathbf{W}(s) = \begin{bmatrix} W_s(s) & 0 & 0 \\ 0 & W_s(s) & 0 \\ 0 & 0 & W_s(s) \end{bmatrix} \tag{5.1}$$

where

$$W_s(s) = \frac{s/M + \omega_0}{s + \omega_0 A_w}$$

The values are

$$M = 5, \ A_w = 0.09, \ \omega_0 = 0.8,$$

where A is the maximum allowed steady state offset, ω_0 is the desired bandwidth and M is the sensitivity peak. Regarding the controller, the inverse of $\mathbf{W}_s$ affects the desired sensitivity loop shape in its upper bound. The inverse of the gain $\mathbf{W}_{ks}$ limits the controller output u.

Applying the theory from Section 4.3.1, the H_∞ norm γ in both pole placement and LQR control models are $\gamma_{\text{Pole Placement}} = 0.3678$, $\gamma_{\text{LQR}} = 0.3602$, respectively.

In the case of robustifying the system through H_∞ loop shaping, the goal is to find a pre-weighting and optional post-pre-weighting using the theory shown in Section 4.3.2. Therefore, we need to choose a loop gain that has a rapid attenuation of the gain at high frequencies making the feedback system less sensitive to measurement noise and to unmodelled dynamics. Integral control plays an important role in control system design because it ensures asymptotic tracking and disturbance rejection when the exogenous signals are constant or asymptotically approach constant limits. It is robust to plant parametric uncertainties, in the sense that asymptotic tracking and disturbance rejection will take place for any uncertainty that preserves the stability of the closed-loop system [Kha00]. In this case, using the Tuning Control Toolbox of Matlab we chose a PI controller for the shape. We selected this controller because it has a good response for static performance:

$$W_e(s) = P + I \left[\frac{1}{s} \right]$$

The values of the parameters are $P = 17.88$ and $I = 78.85$. Then, the value of the

norm in both pole placement and LQR control models are $\varepsilon_{\text{Pole Placement}} = 2.4489$, $\varepsilon_{\text{LQR}} = 1.7600$, respectively. The responses are shown in Figures 5.7 and 5.8.
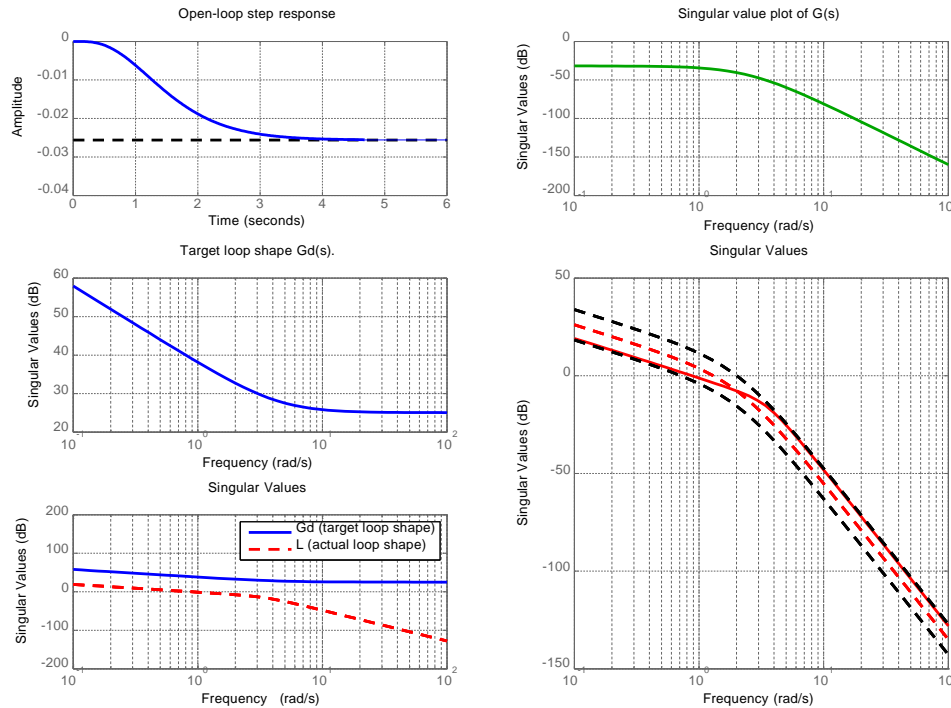
Figure 5.7: System response with Pole Placement Control and H_∞ Loop Shaping Robustification.

5.2.2 System Characteristics

The gantry crane system is located at the Laboratory of Automation and Systems Engineering at Computer Science and Automation Department, Technische Universität Ilmenau. The structure of the experiment is shown in Figure 5.9. The dimensions of the structure in length, width and height are 2m, 1.54m and 1.4m, respectively. Based on these values, two situations have been tested to analyze the response of the system to external perturbations.

System in Fixed Position

In this condition, the payload is located in the middle of the structure, the position of the coordinates in $z_1 = 1m$, $z_2 = 0.77m$, and $z_3 = -0.7m$. The goal of this test is to observe the effect of the disturbance in the trolley and the payload and analyze the
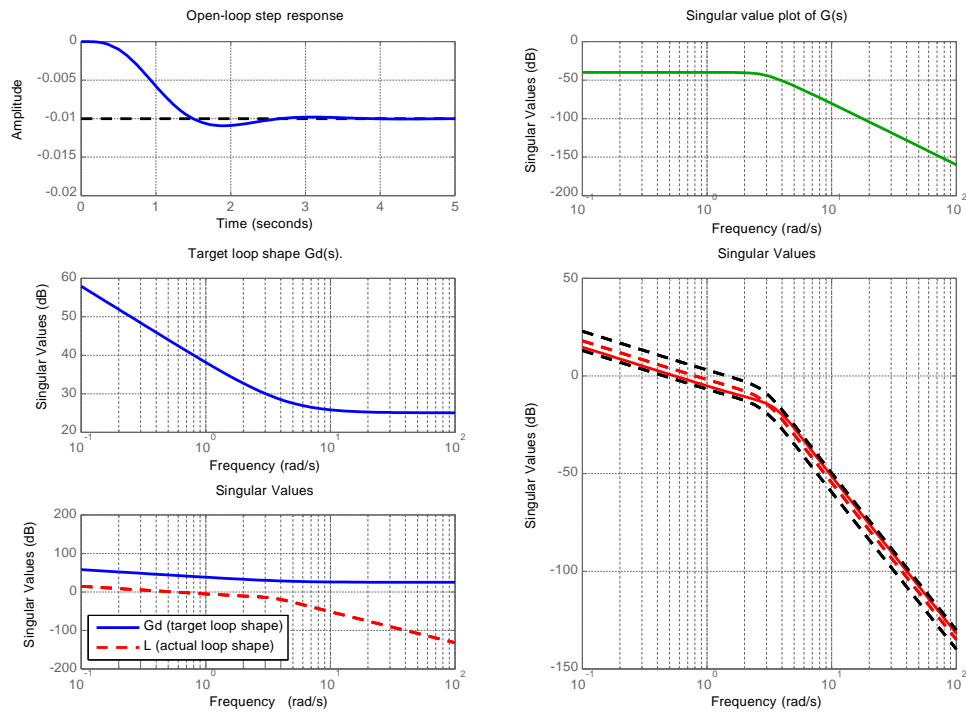
Figure 5.8: System response with LQR Control and H_∞ Loop Shaping Robustification.
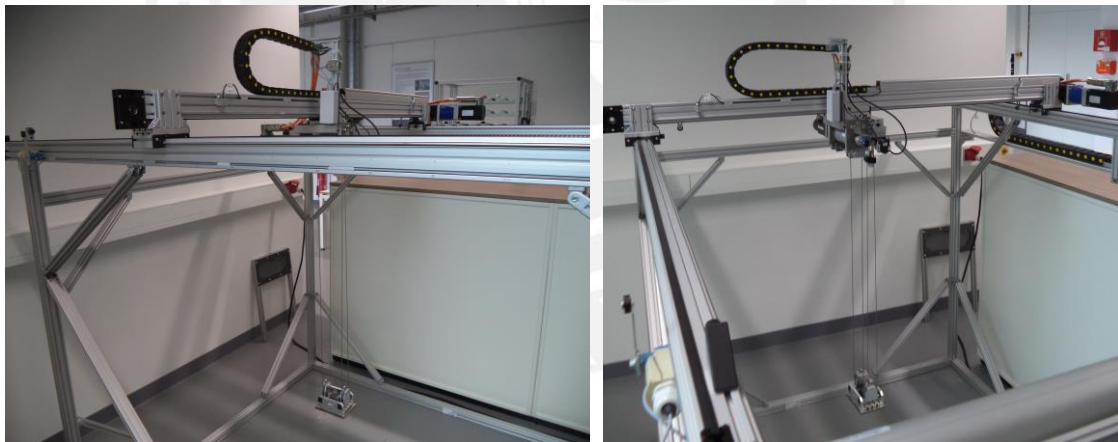
Figure 5.9: Gantry Crane System

effect in the final position of the payload. The disturbances presented here is a unit step in the direction of α in the first 6 sec and β in 12 sec. This disturbances represents the effects of changes in the angular acceleration of the angles. The position of the payload is shown in Figure 5.10.
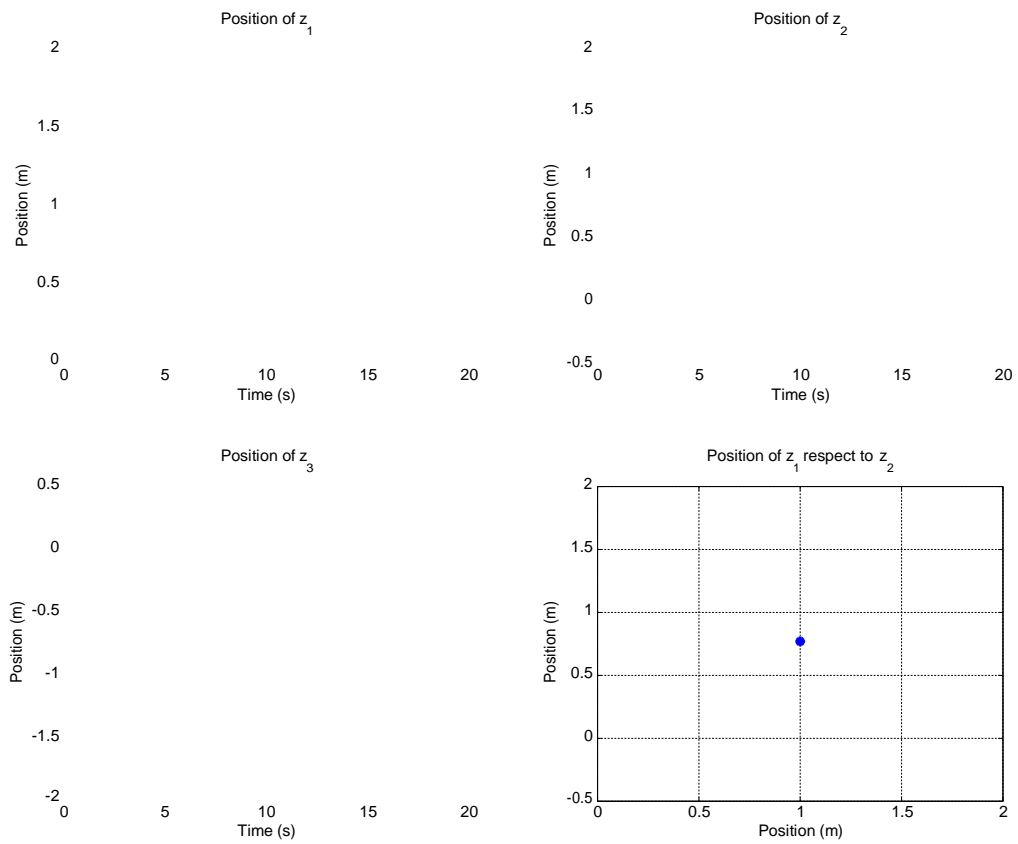
Figure 5.10: Fixed Position Error of the System with Pole Placement.
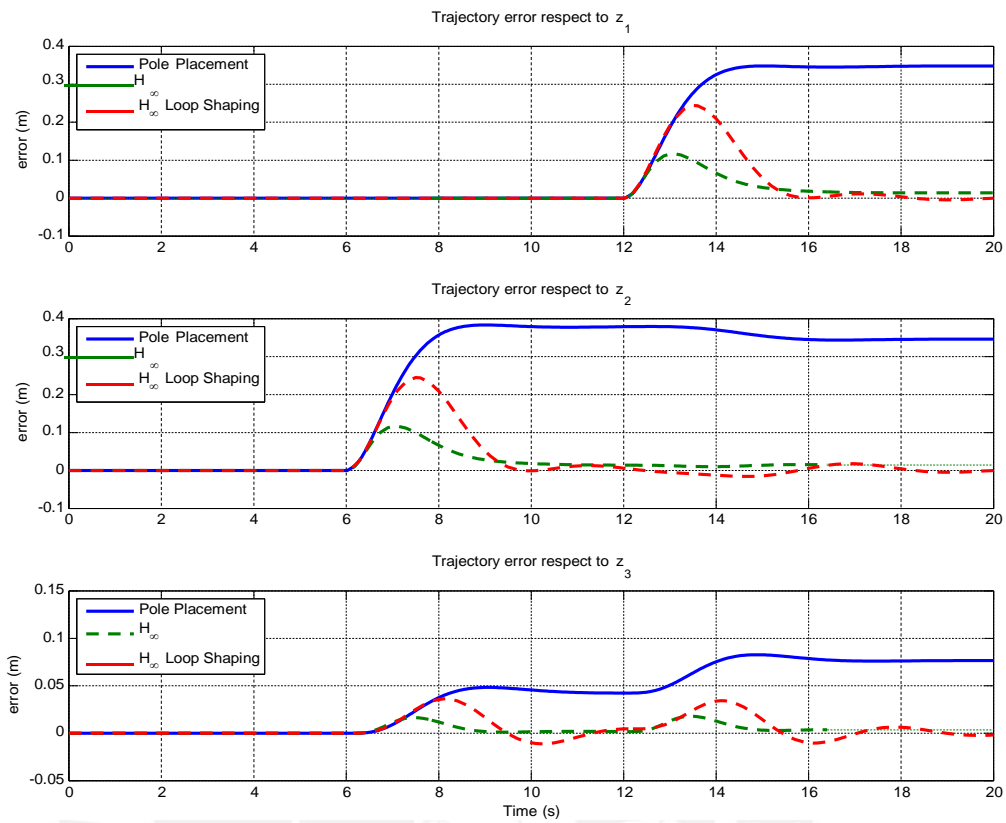
Figure 5.11: Fixed Position Error of the System with Pole Placement.
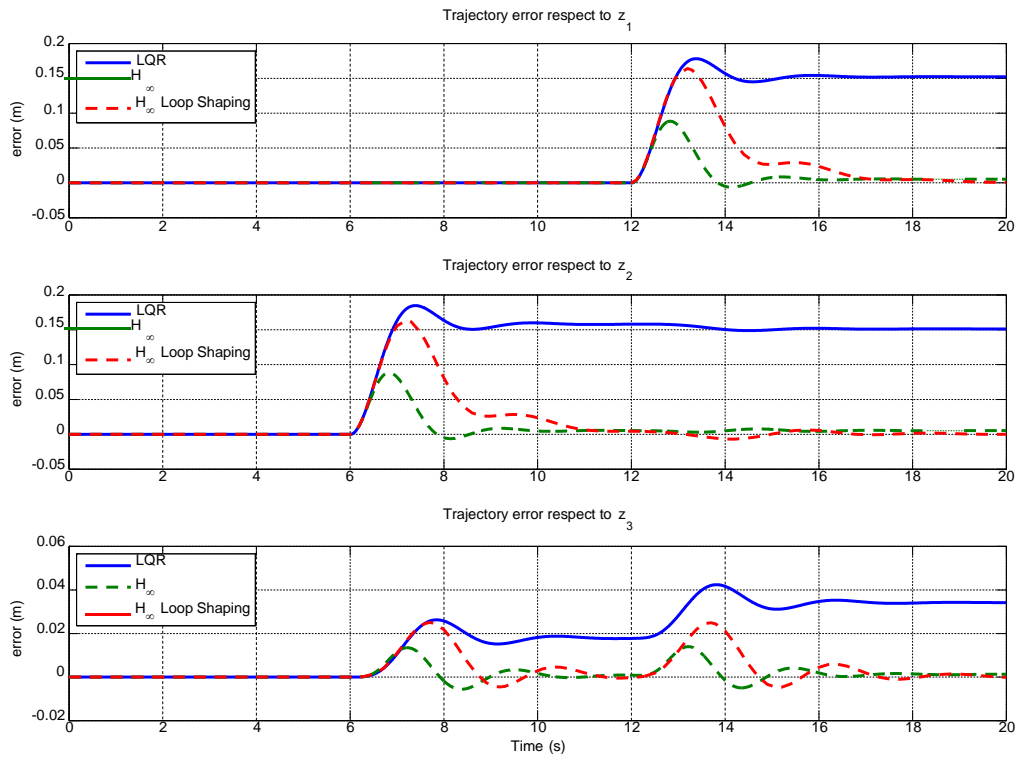
Figure 5.12: Fixed Position Error of the System with LQR.
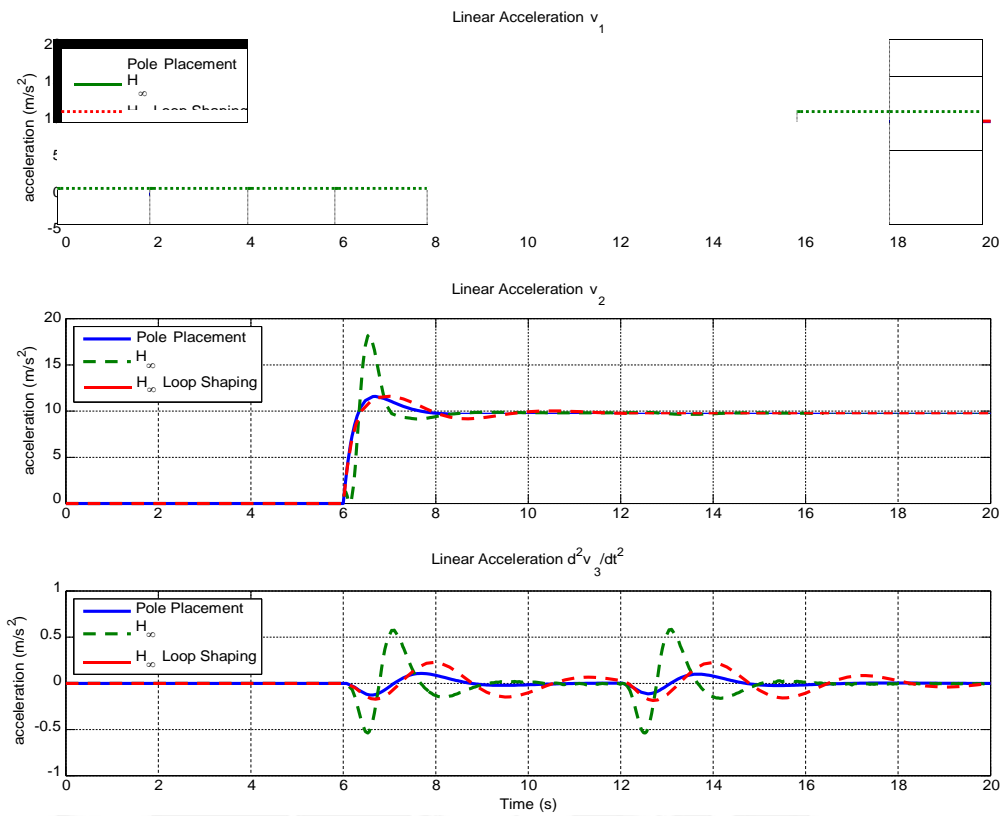
Figure 5.13: Fixed Position Linear Acceleration of the System with Pole Placement.
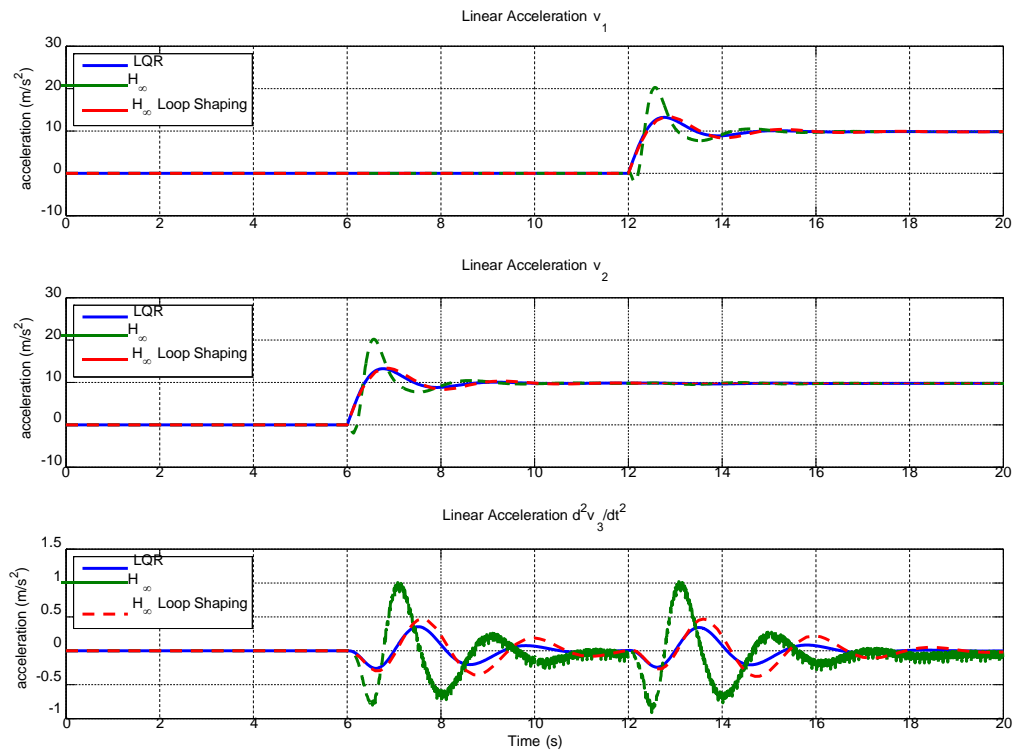
Figure 5.14: Fixed Position Linear Acceleration of the System with LQR.
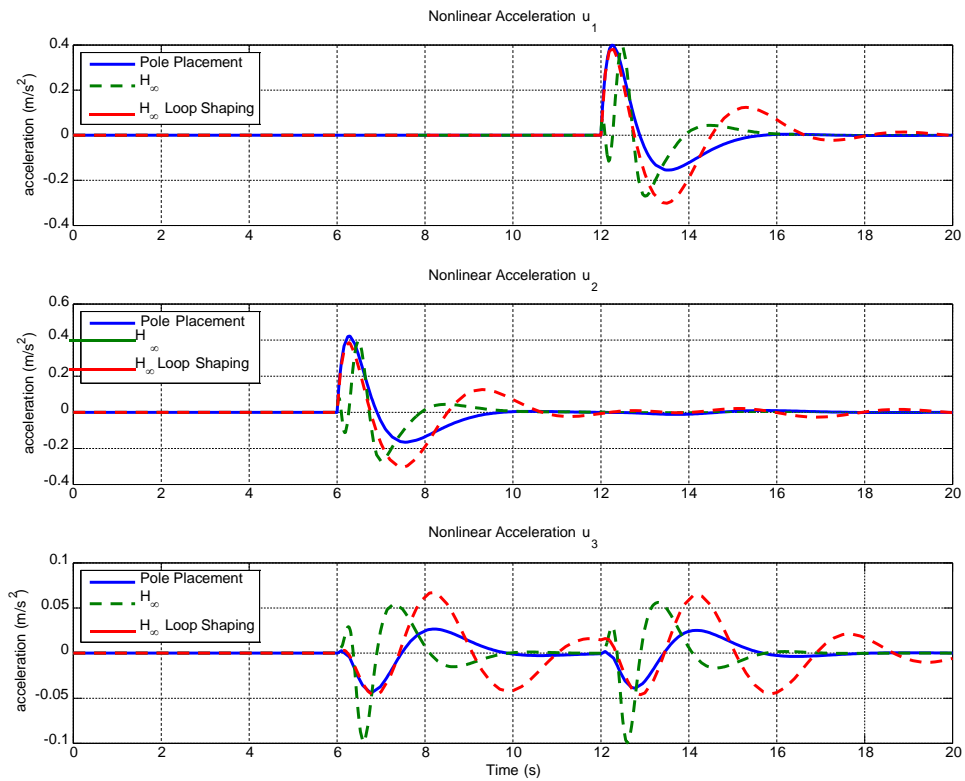
Figure 5.15: Fixed Position NonLinear Acceleration of the System with Pole Placement.
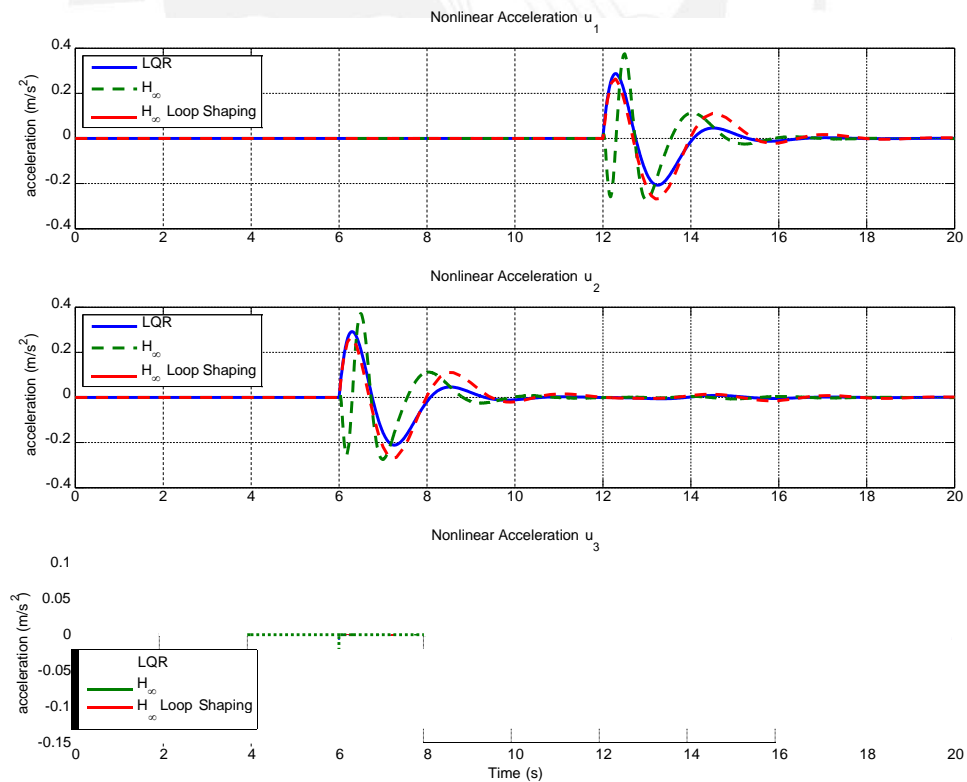
Figure 5.16: Fixed Position NonLinear Acceleration of the System with LQR.
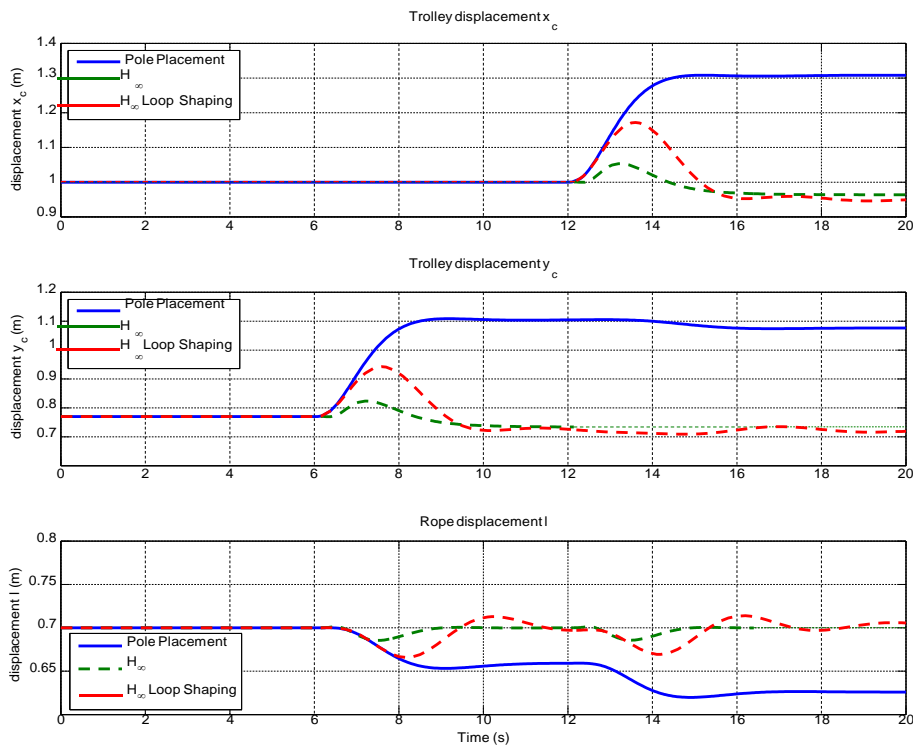
Figure 5.17: Fixed Position of the Trolley of the System with Pole Placement.
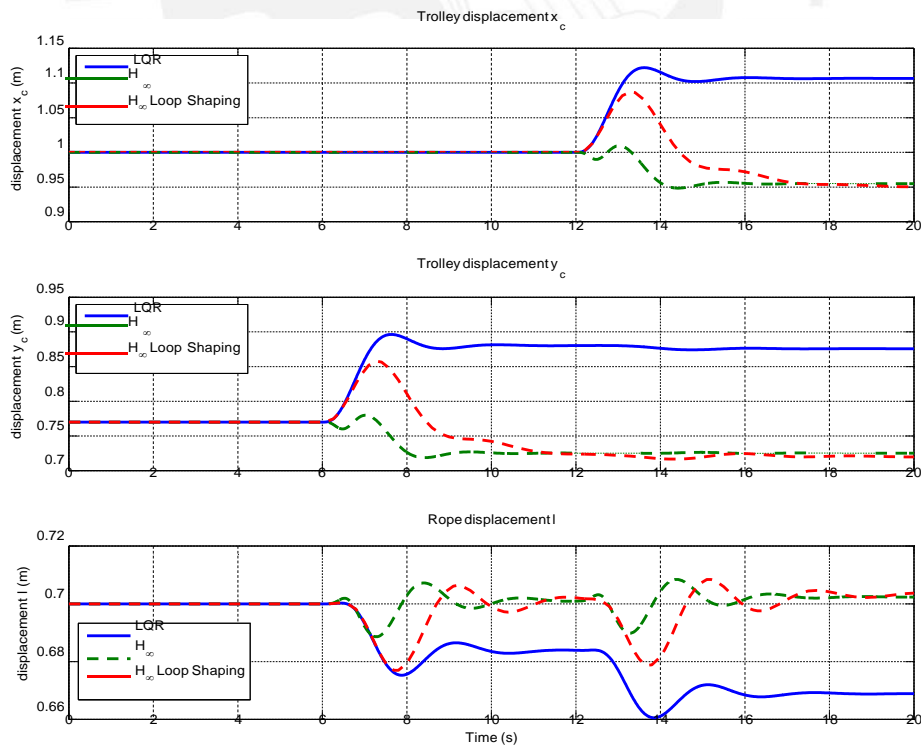
Figure 5.18: Fixed Position of the Trolley of the System with LQR.
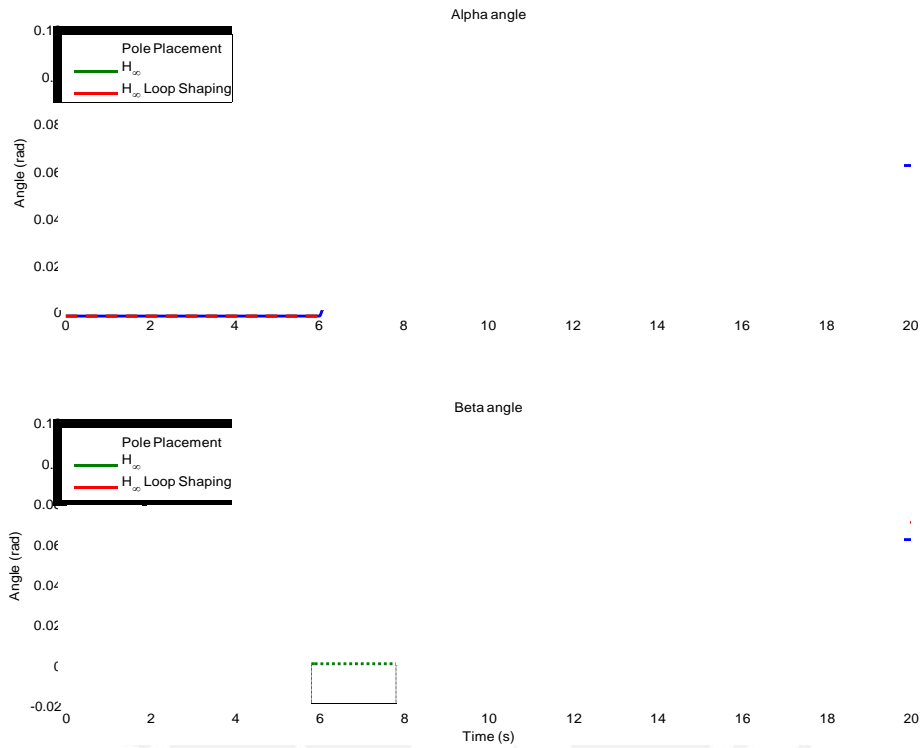
Figure 5.19: Fixed Position angles with Pole Placement.
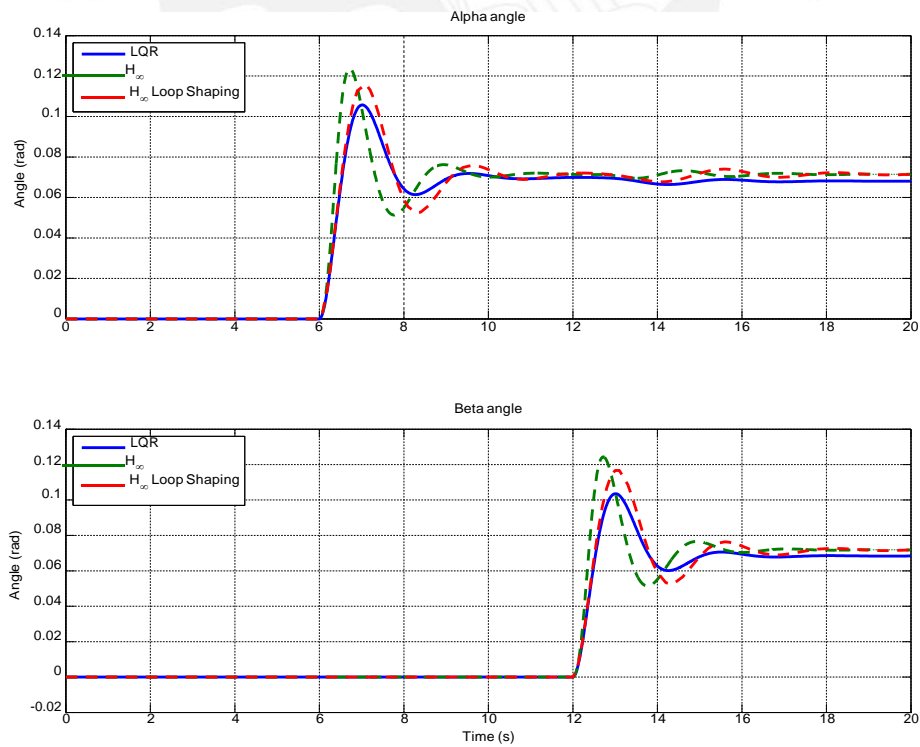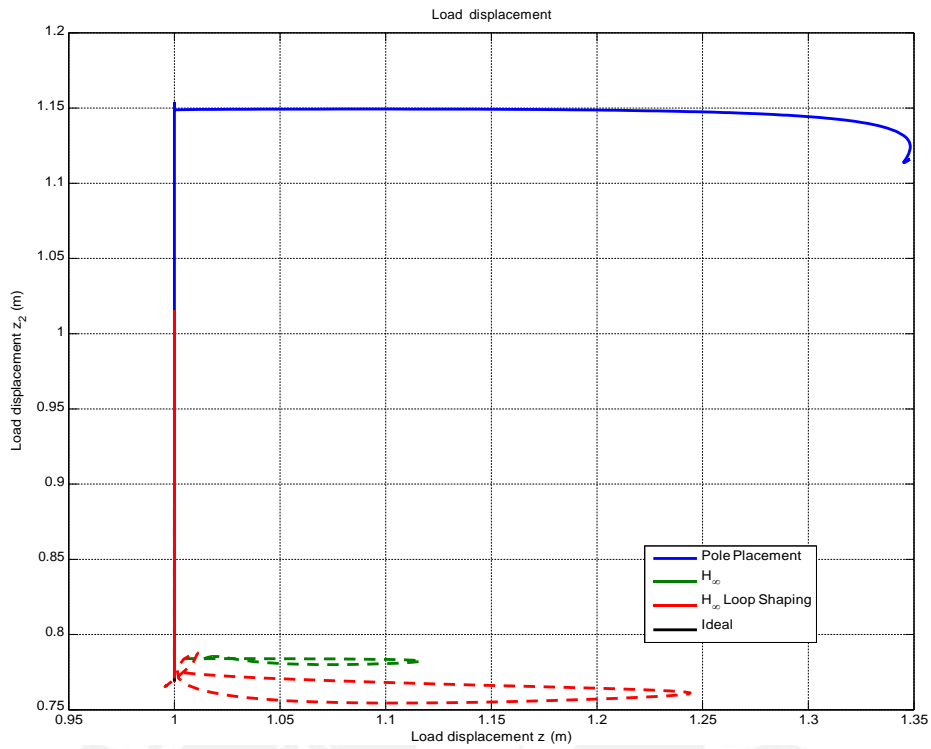

Figure 5.20: Fixed Position angles of the System with LQR.
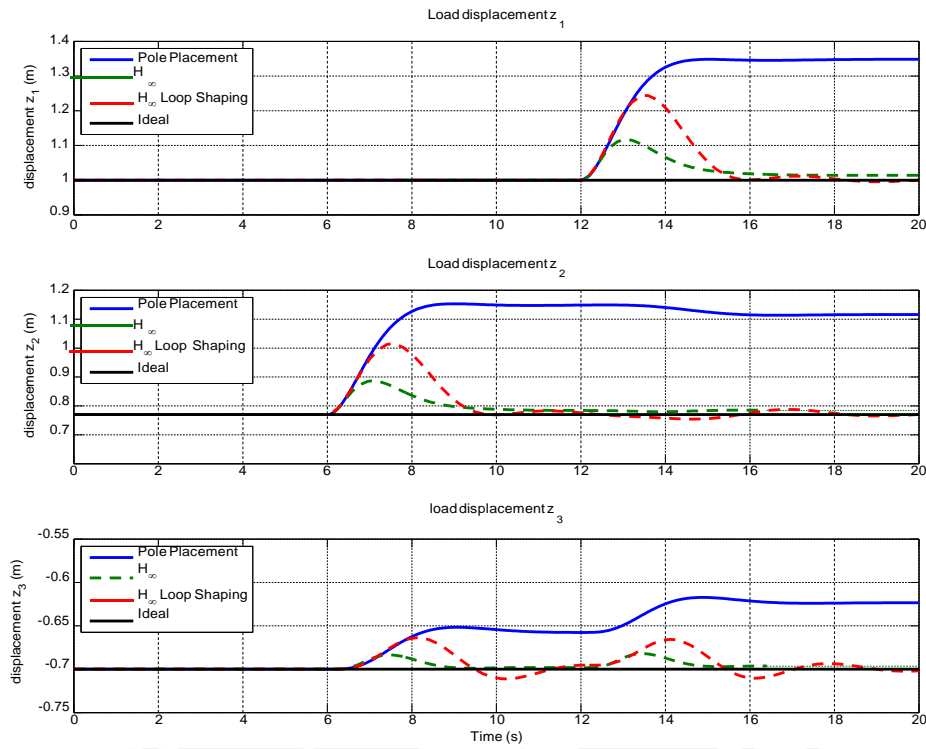
Figure 5.21: Fixed Position Load Displacement with Pole Placement.
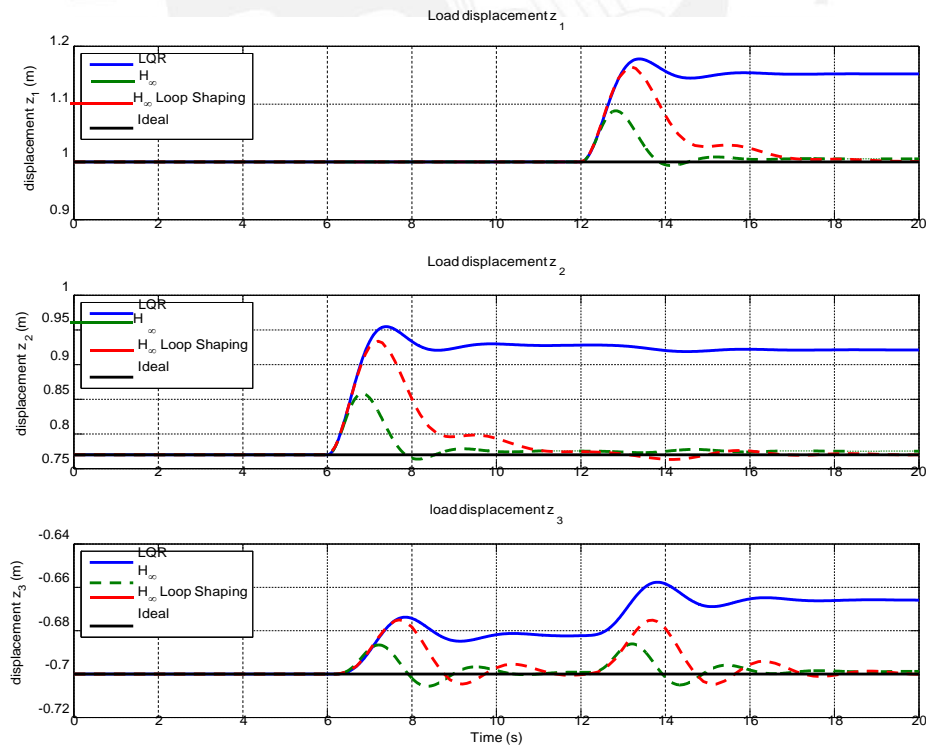
Figure 5.22: Fixed Position Load Displacement with LQR.
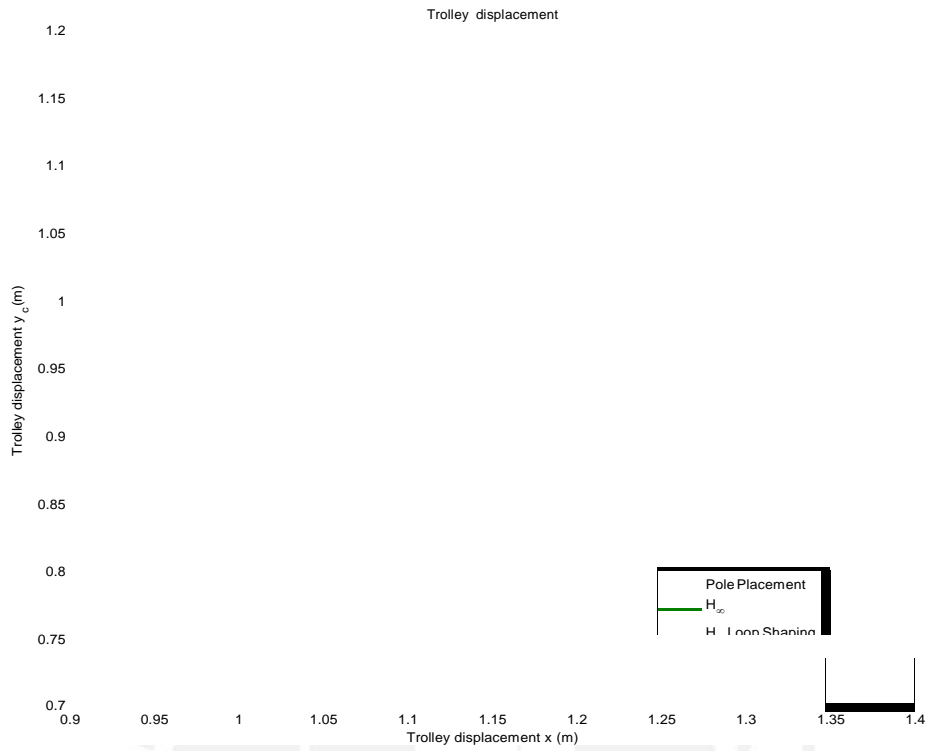
Figure 5.23: Fixed Position Trolley Displacement in *x-y* with Pole Placement.
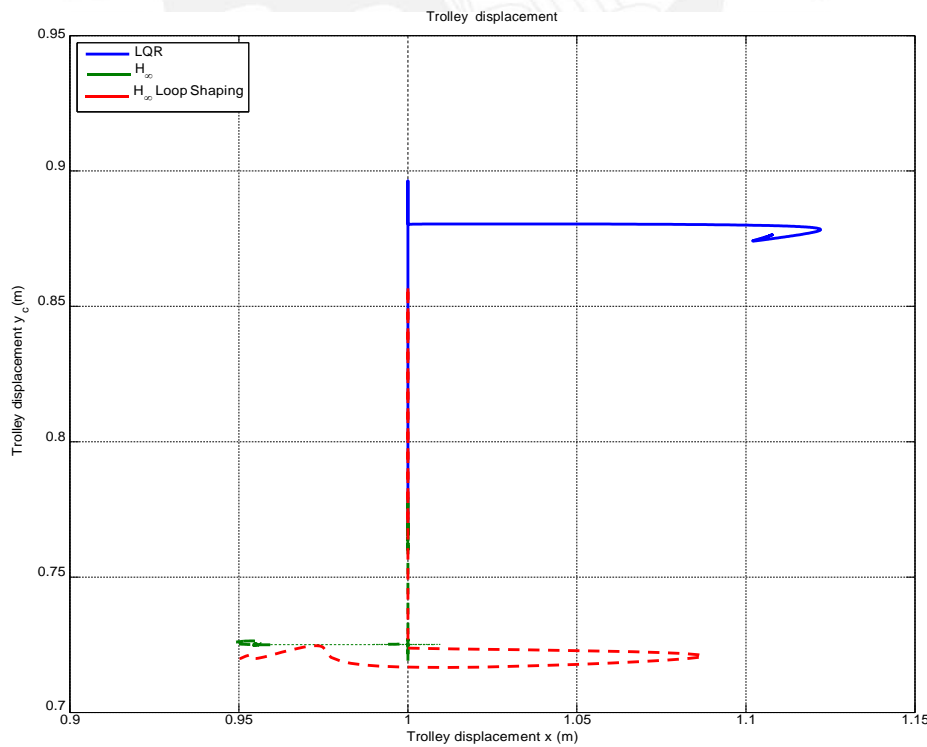
Figure 5.24: Fixed Position Trolley Displacement in *x-y* with LQR.

Figure 5.25: Fixed Position Load Displacement in z_1-z_2 with Pole Placement.
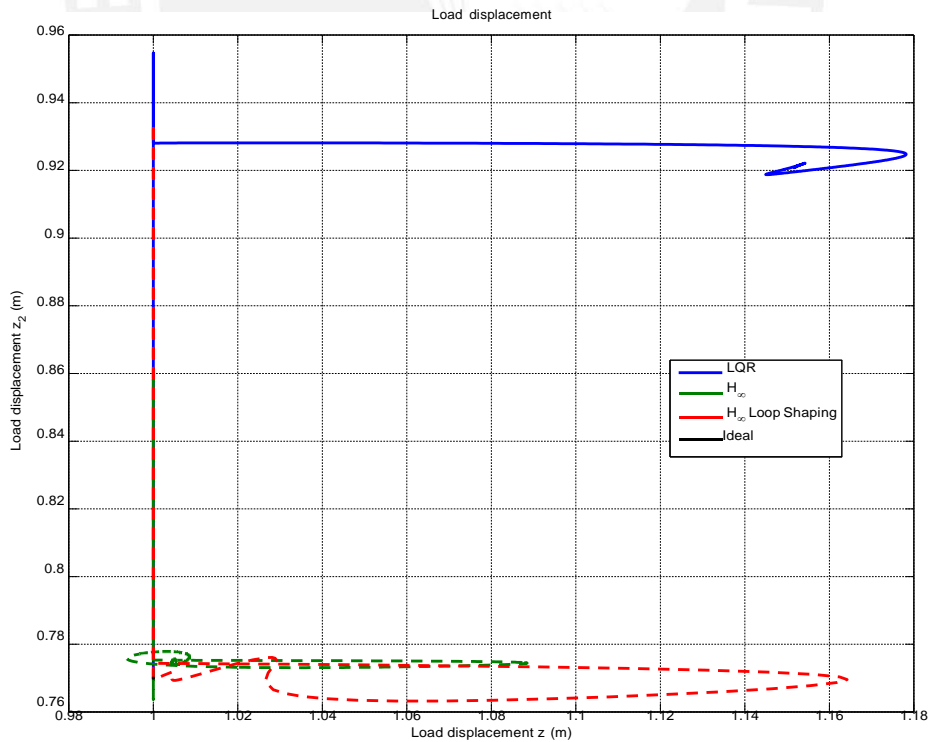

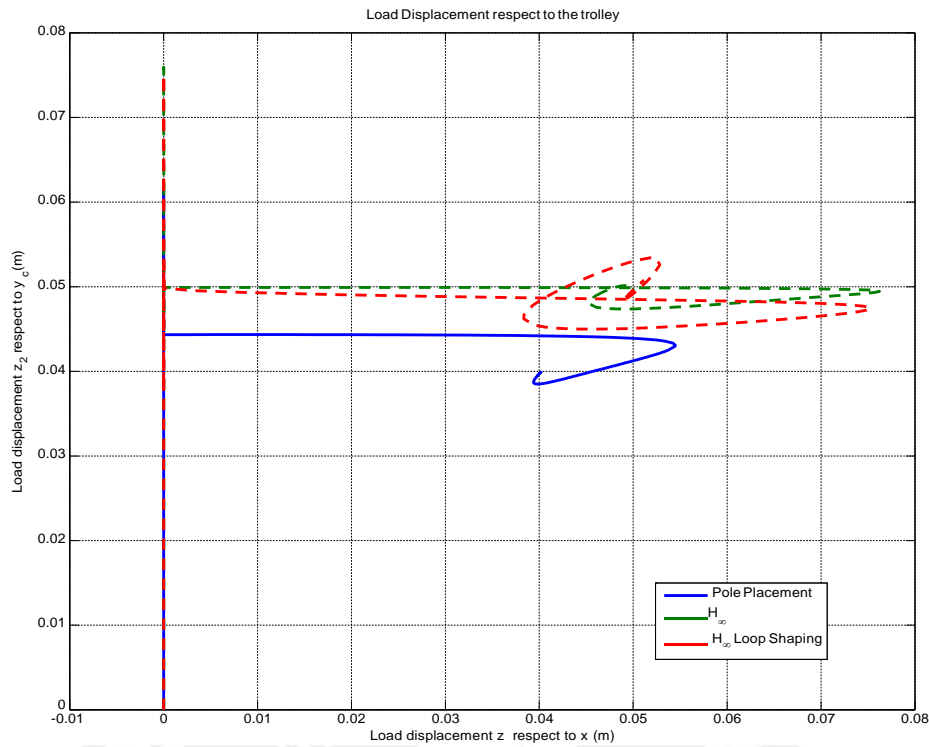Figure 5.26: Fixed Position Load Displacement in z_1-z_2 with LQR.

Figure 5.27: Fixed Position Load Displacement in z_1-z_2 respect to the Trolley with Pole Placement.

In order to analyse the behaviour of the system in this condition, both tables 5.1 and 5.2 about maximun acceleration of the trolley and the final position of the load due to disturbances have been development and we can show the results in detail.

Control Type	Robustification Type	$\ddot{x}_c$	$\ddot{y}_c$	$\ddot{l}$
	-	0.3995	0.4222	-0.0386
Pole Placement	H_∞	0.3959	0.3960	-0.0993
	H_∞ Loop Shaping	0.3811	0.3864	-0.0461
	-	0.2874	0.2918	-0.0561
LQR	H_∞	0.3746	0.3719	-0.1257
	H_∞ Loop Shaping	0.2639	0.2644	-0.0589

Table 5.1: Maximum Acceleration of the Trolley and the Rope in a Fixed Position (m/s^2).

Table 5.1 shows that the best response of the system with disturbances is when the crane is controlled by LQR and robustified using H_∞ Loop Shaping, in this case the reaction of the accelerations in the trolley have a low value, it means that the effort to control the system is compensated by the acceleration of the rope and we can avoid
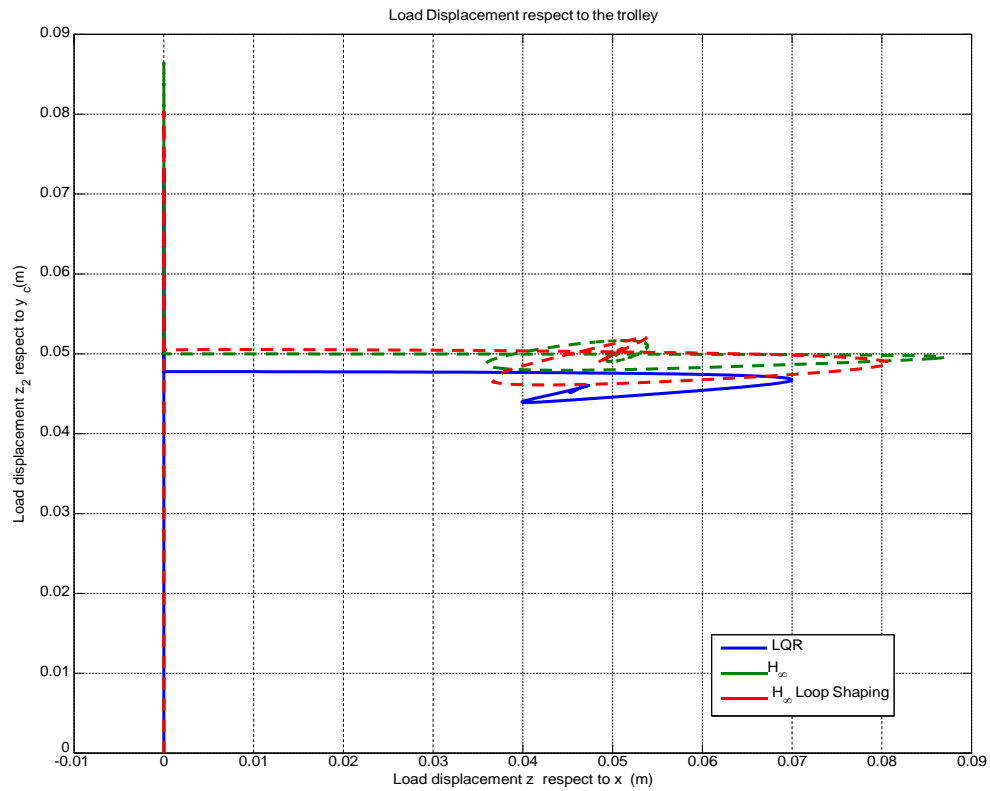
Figure 5.28: Fixed Position Load Displacement in z_1-z_2 respect to the Trolley with LQR.

high peak in the motors of the crane.

Control Type	Robustification Type	z_{1_i}	z_{2_i}	z_{3_i}	z_{1_f}	z_{2_f}	z_{3_f}
Pole Placement	-	1	0.77	-0.7	1.34	1.12	-0.62
	H_∞	1	0.77	-0.7	1.01	0.78	-0.69
	H_∞ Loop Shaping	1	0.77	-0.7	1	0.77	-0.7
LQR	-	1	0.77	-0.7	1.15	0.92	-0.67
	H_∞	1	0.77	-0.7	1.01	0.78	-0.69
	H_∞ Loop Shaping	1	0.77	-0.7	1	0.77	-0.7

Table 5.2: Initial and Final Position of the Payload due to disturbances in a Fixed Position (*m*).

In Table 5.2 again we can see that the best performance in the system is with LQR control and H_∞ robustification because the payload stay in the same position after the disturbances. However, as we can see in the Figures 5.26 and 5.28, there is a overslope when the load try to adjust its position. This behaviour can be fixed testing new weight values in the Loop Shaping algorithm.

System in a Settled Trajectory

In this condition, the payload is displaced from an inital position to a final place following a trajectory. The position of the coordinates in the initial position is $z_1 = 0.1m$, $z_2 = 0.1m$ and $z_3 = -0.15m$. The final place is located at $z_1 = 0.6m$, $z_2 = 0.77m$ and $z_3 = -0.7m$ following a line trajectory in the first $10\,sec$, then the payload follows a circular path until its final position for another $10\,sec$ to complete the settled path. The goal of this test is to observe the effect of the disturbance in the trolley and the payload in motion on the final position of the payload reaching the goal place. The disturbances, as in the previous test, is a unit step in the direction of α in the first $6\,sec$ and β in $12\,sec$. In this case, both reactions occur seconds before and after the change of the path. The trajectory of the payload is shown in Figure 5.29.
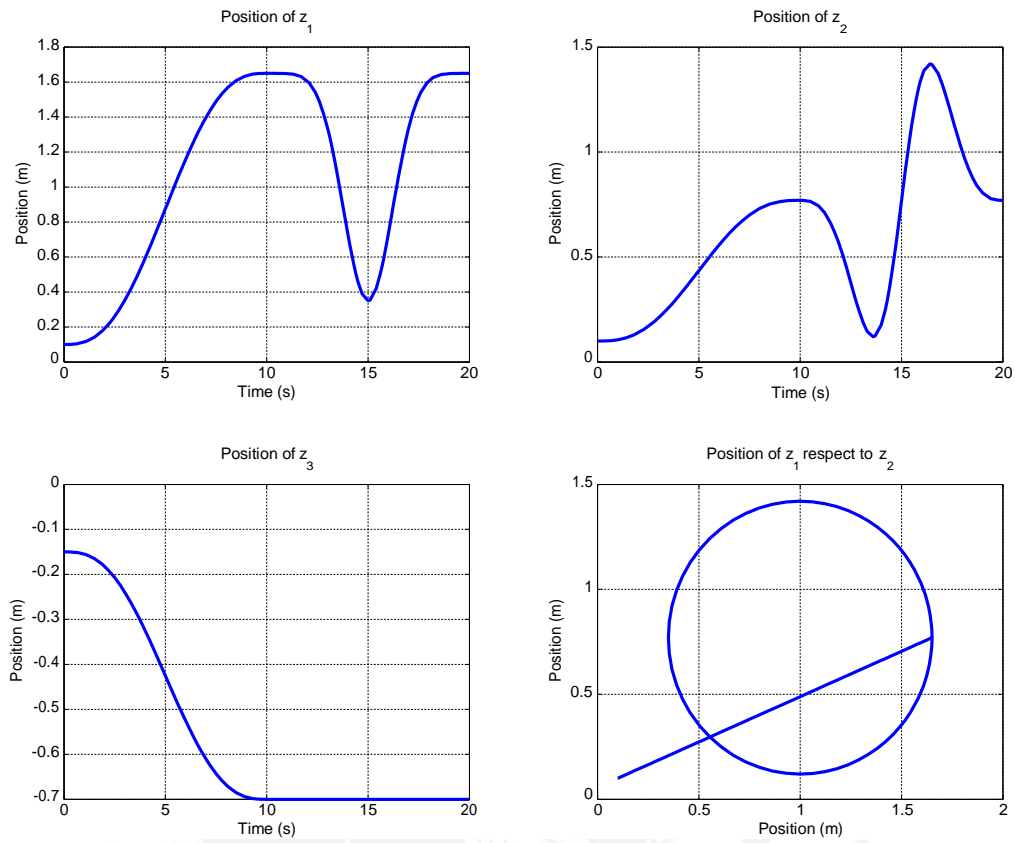
Figure 5.29: Fixed Position Error of the System with Pole Placement.
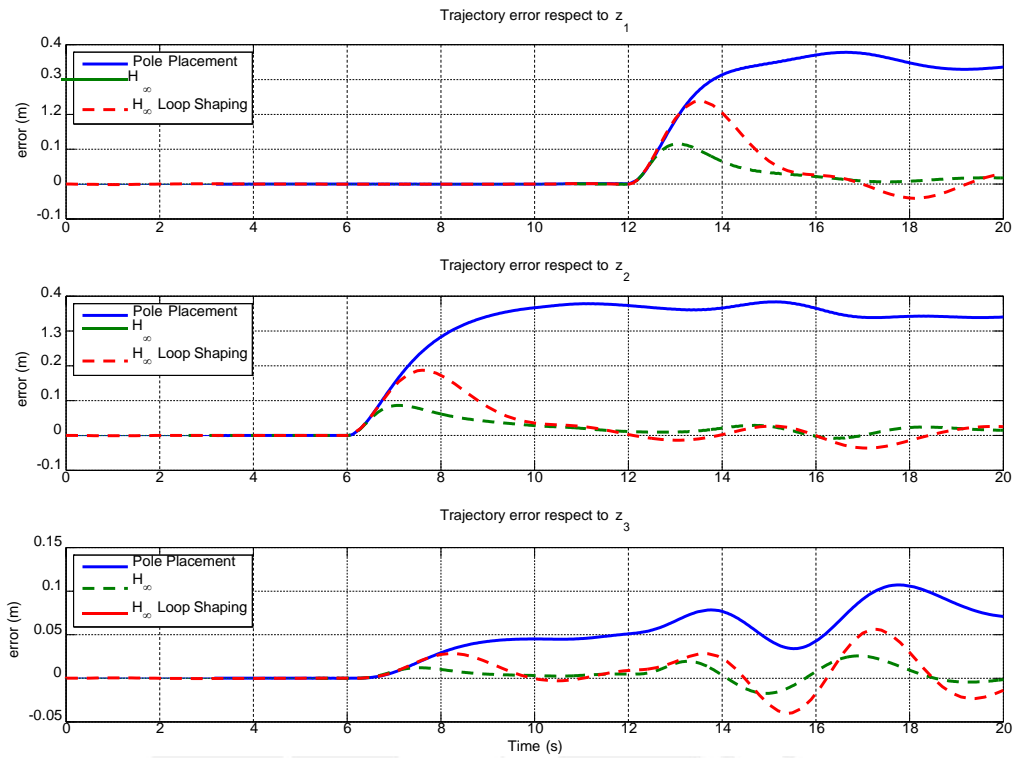
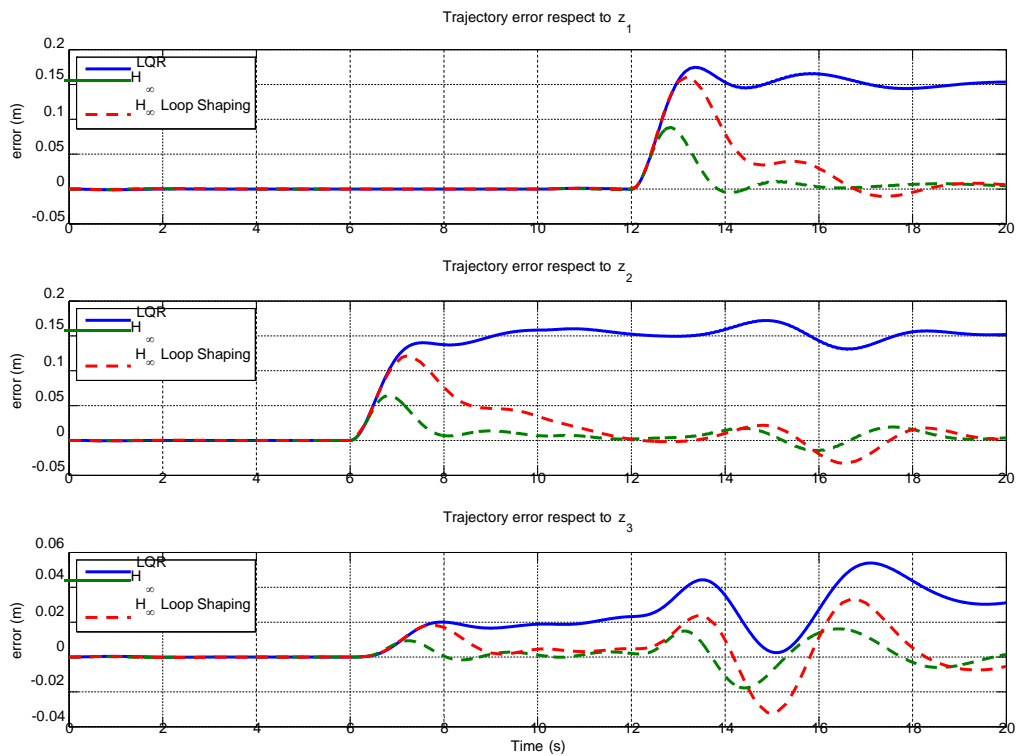Figure 5.30: Settled Trajectory Error of the System with Pole Placement.

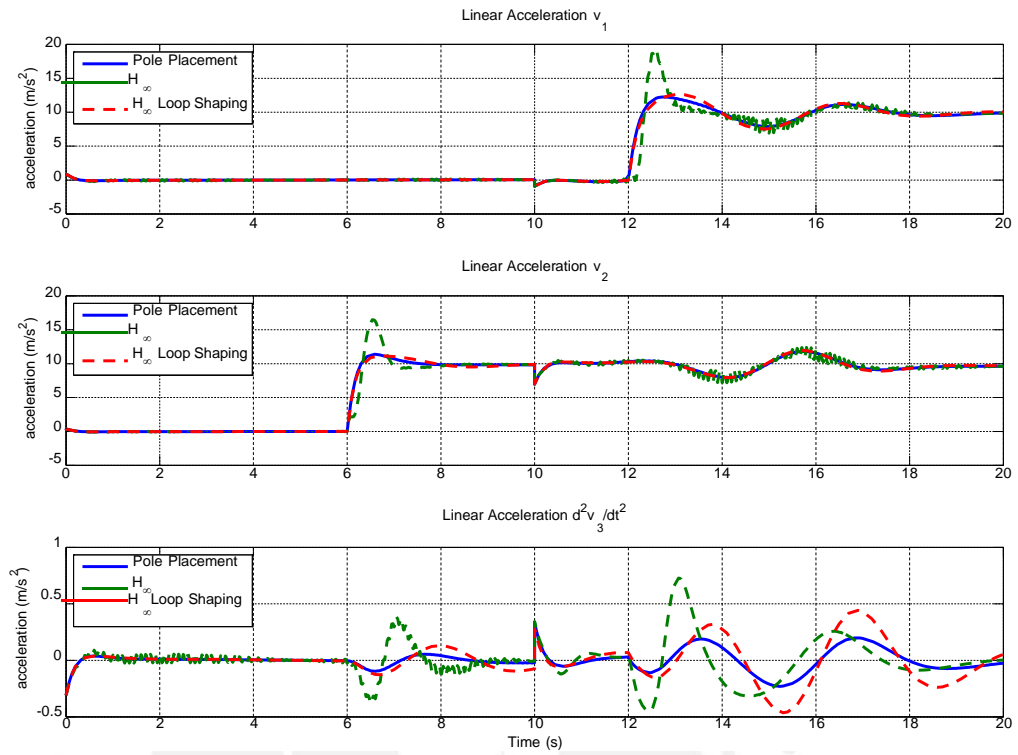Figure 5.31: Settled Trajectory Error of the System with LQR.

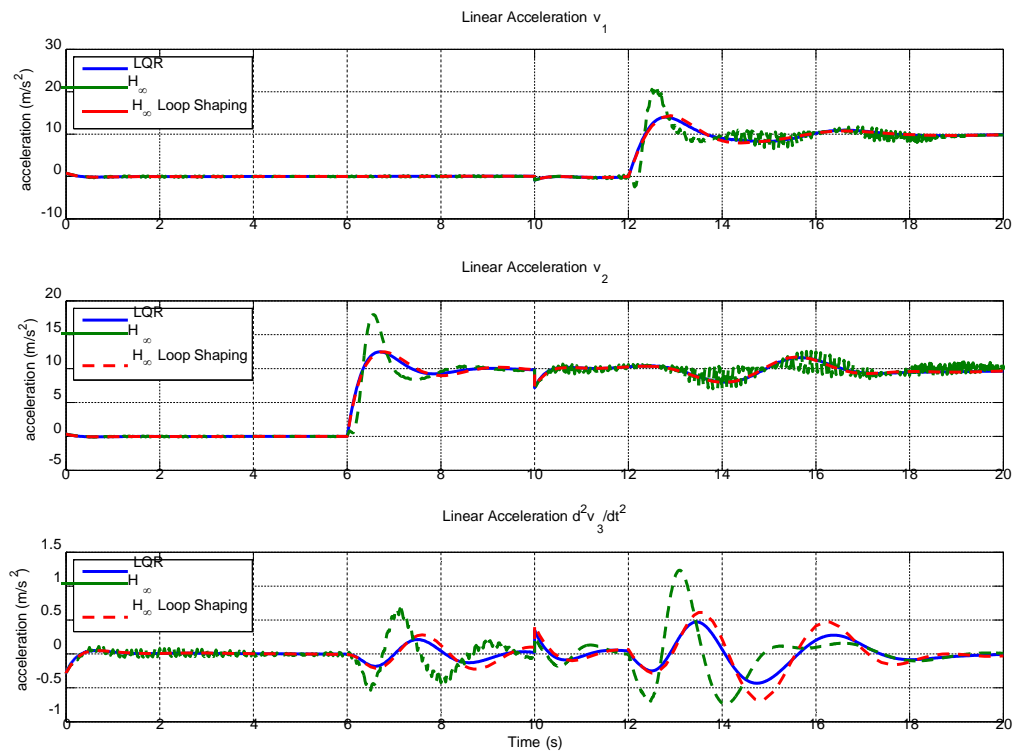Figure 5.32: Settled Trajectory Linear Acceleration of the System with Pole Placement.

Figure 5.33: Settled Trajectory Linear Acceleration of the System with LQR.
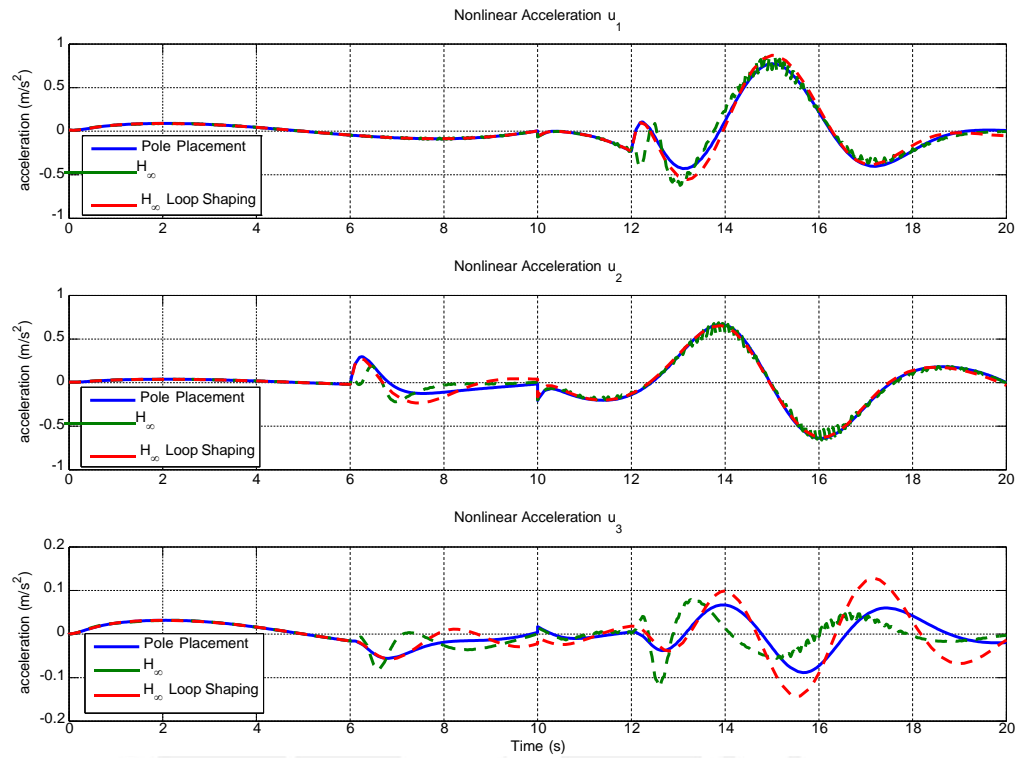
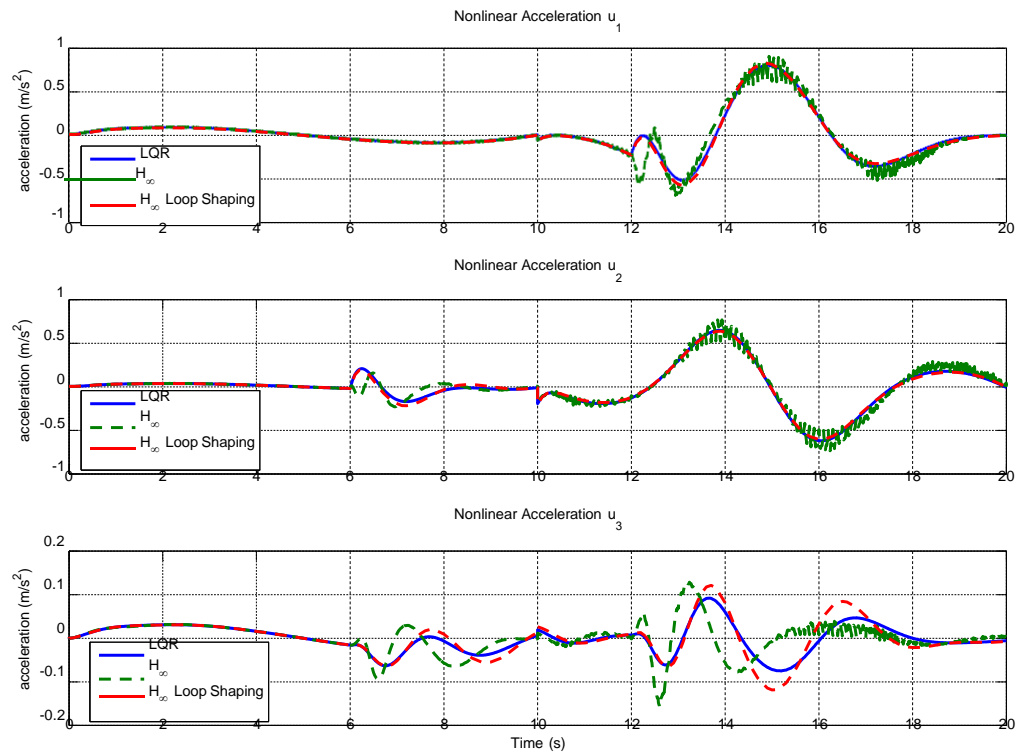Figure 5.34: Settled Trajectory NonLinear Acceleration of the System with Pole Placement.

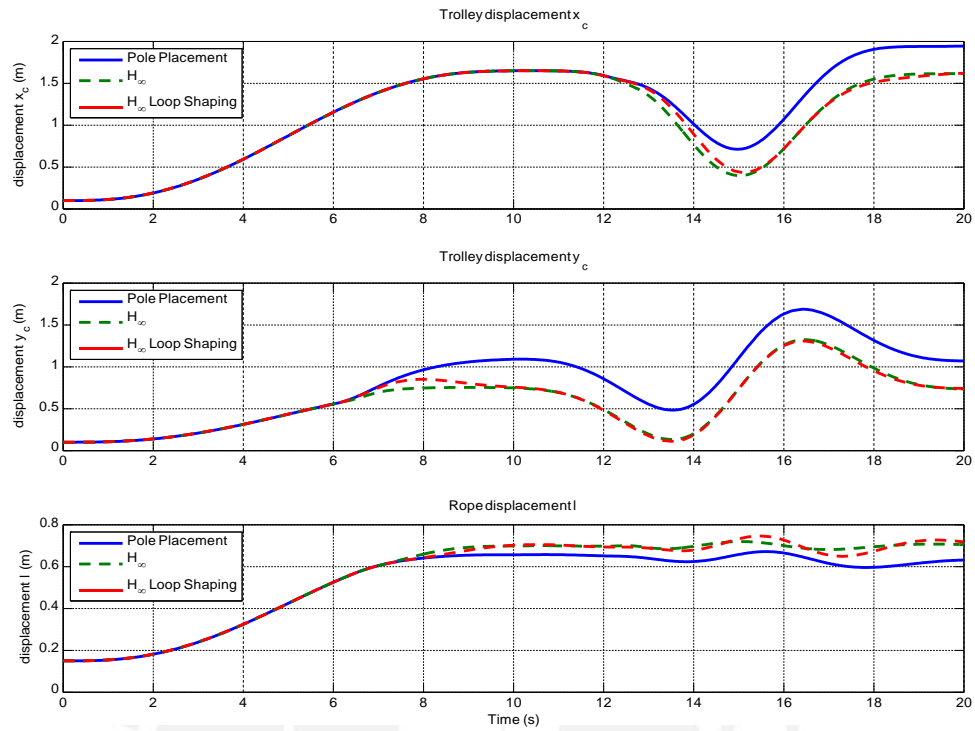Figure 5.35: Settled Trajectory NonLinear Acceleration of the System with LQR.

Figure 5.36: Settled Trajectory of the Trolley of the System with Pole Placement.
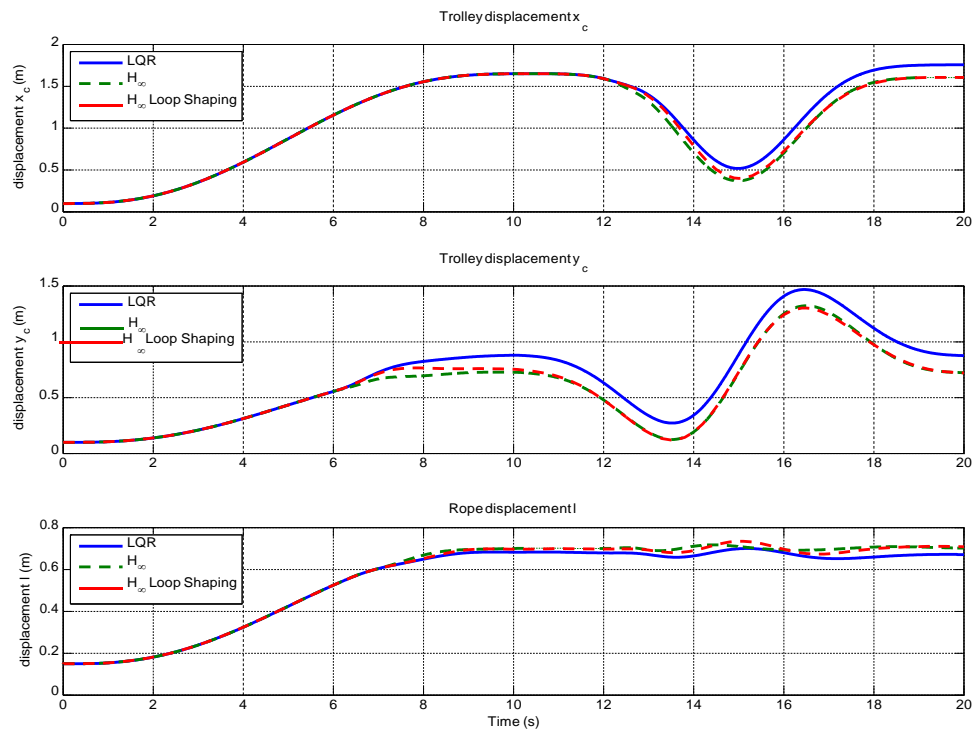

Figure 5.37: Settled Trajectory of the Trolley of the System with LQR.

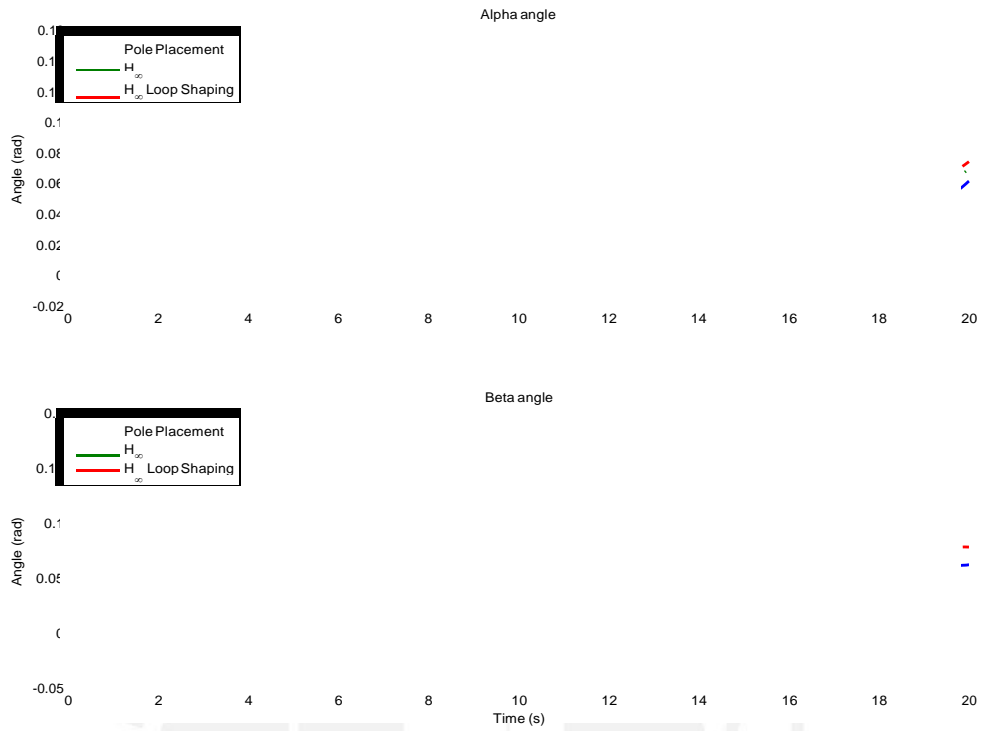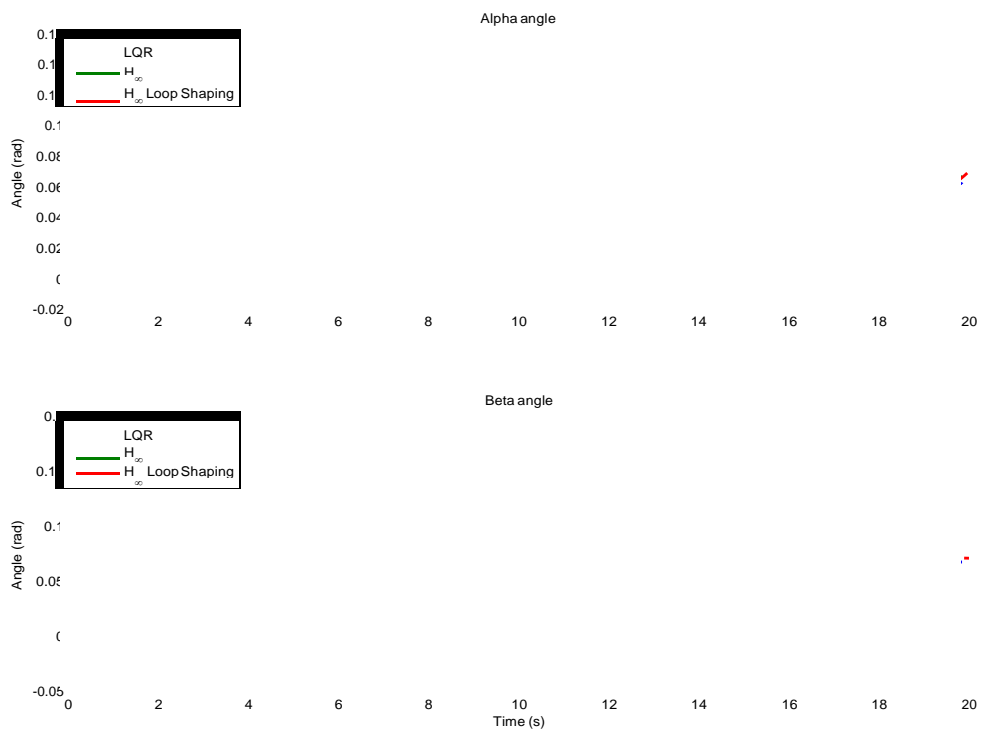Figure 5.38: Settled Trajectory angles with Pole Placement.

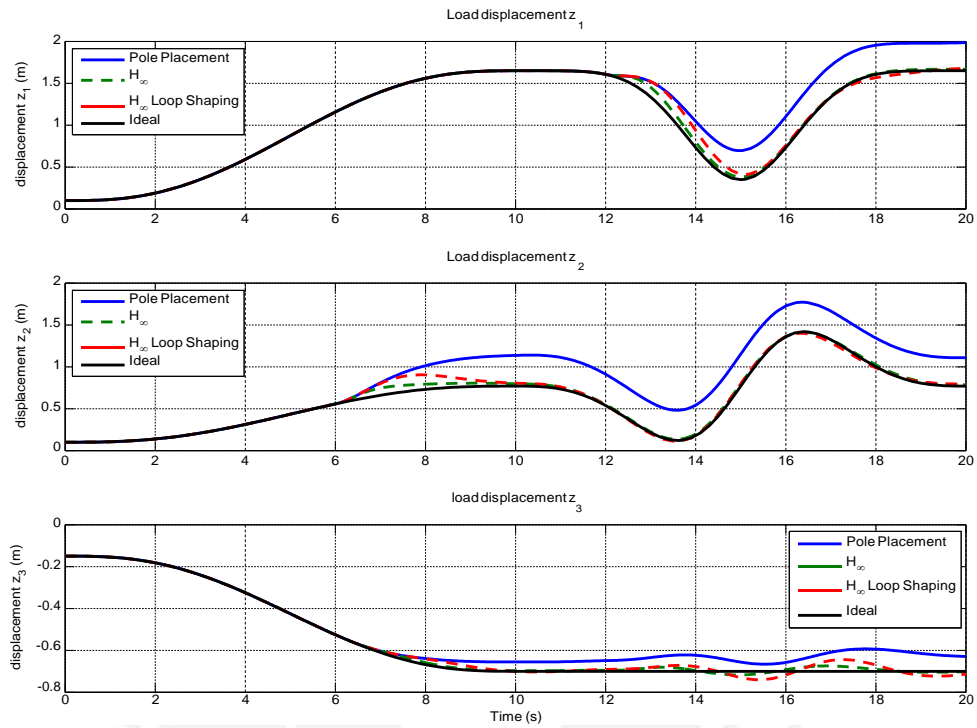Figure 5.39: Settled Trajectory angles of the System with LQR.

Figure 5.40: Settled Trajectory Load Displacement with Pole Placement.
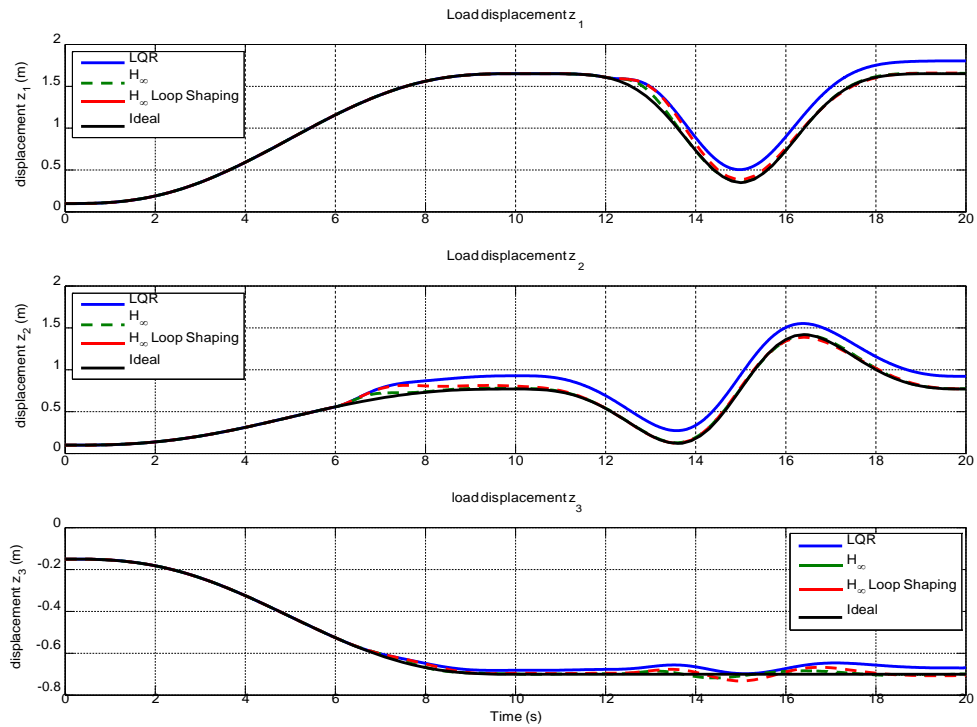

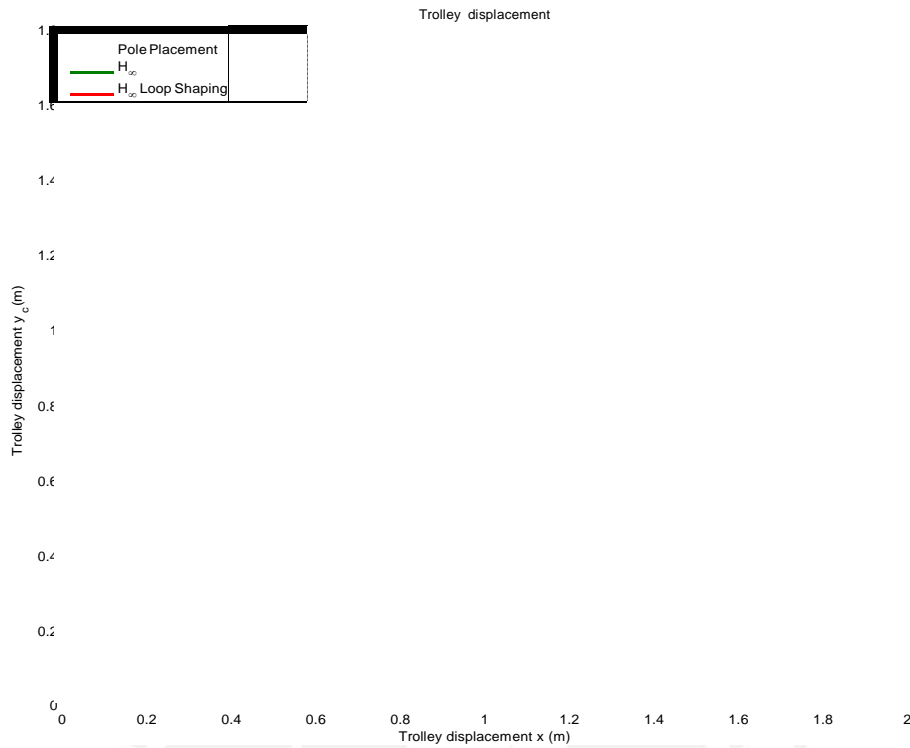Figure 5.41: Settled Trajectory Load Displacement with LQR.

Figure 5.42: Settled Trajectory Trolley Displacement in *x-y* with Pole Placement.
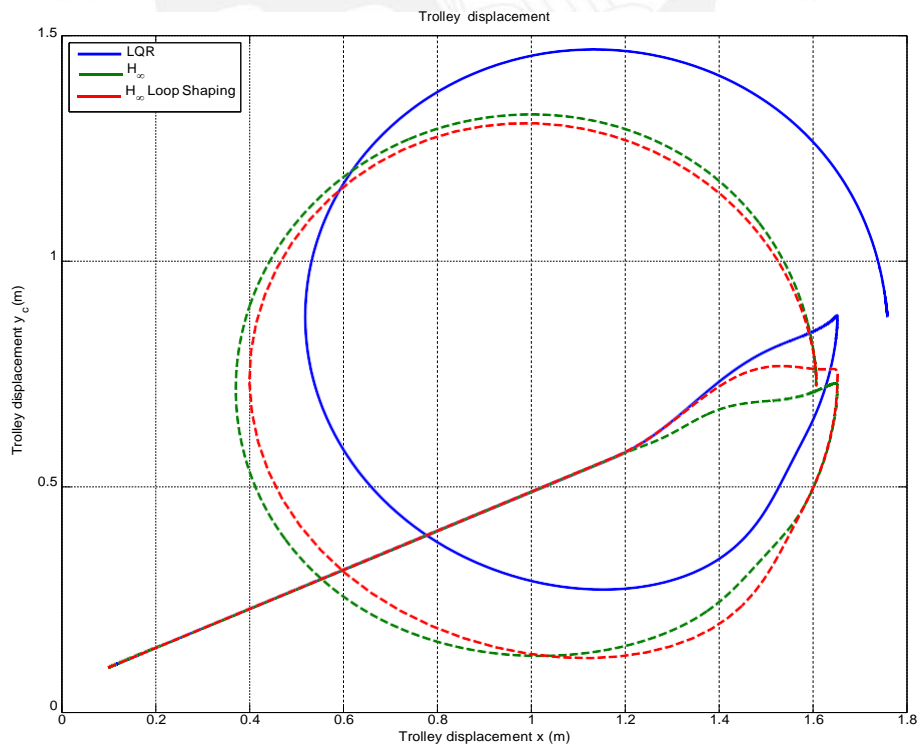
Figure 5.43: Settled Trajectory Trolley Displacement in *x-y* with LQR.
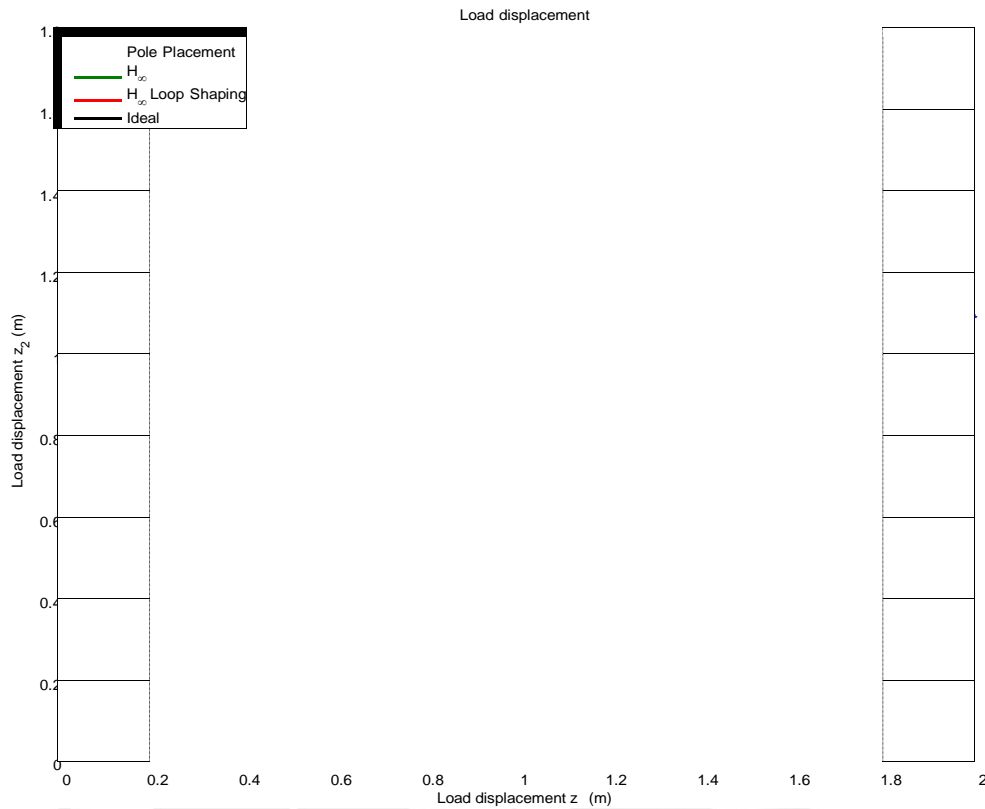
Figure 5.44: Settled Trajectory Load Displacement in z_1-z_2 with Pole Placement.

Tables 5.3 and 5.4 have the values about maximun acceleration of the trolley and the desired position of the load affect by disturbances.

Control Type	Robustification Type	$\ddot{x}_c$	$\ddot{y}_c$	$\ddot{l}$
Pole Placement	-	0.7749	0.6670	0.0667
	H_∞	0.8148	0.6172	-0.1220
	H_∞ Loop Shaping	0.8702	0.6530	-0.1432
LQR	-	0.7903	0.6468	0.0918
	H_∞	0.7417	0.6711	-0.1581
	H_∞ Loop Shaping	0.8258	0.6378	-0.1185

Table 5.3: Maximum Acceleration of the Trolley and the Rope in a Settled Trajectory (m/s^2).

Table 5.3 shows the response of the system with disturbances in this case the values obtained with both controller are are closely similar, However in Figures 5.34 we can see that the signal of the system respect of H_∞. contains noise, therefore, the action to stabilize the trolley make the motors to adjust constantly its position during the circular path. In this case the Loop shaping robustification presents better results.
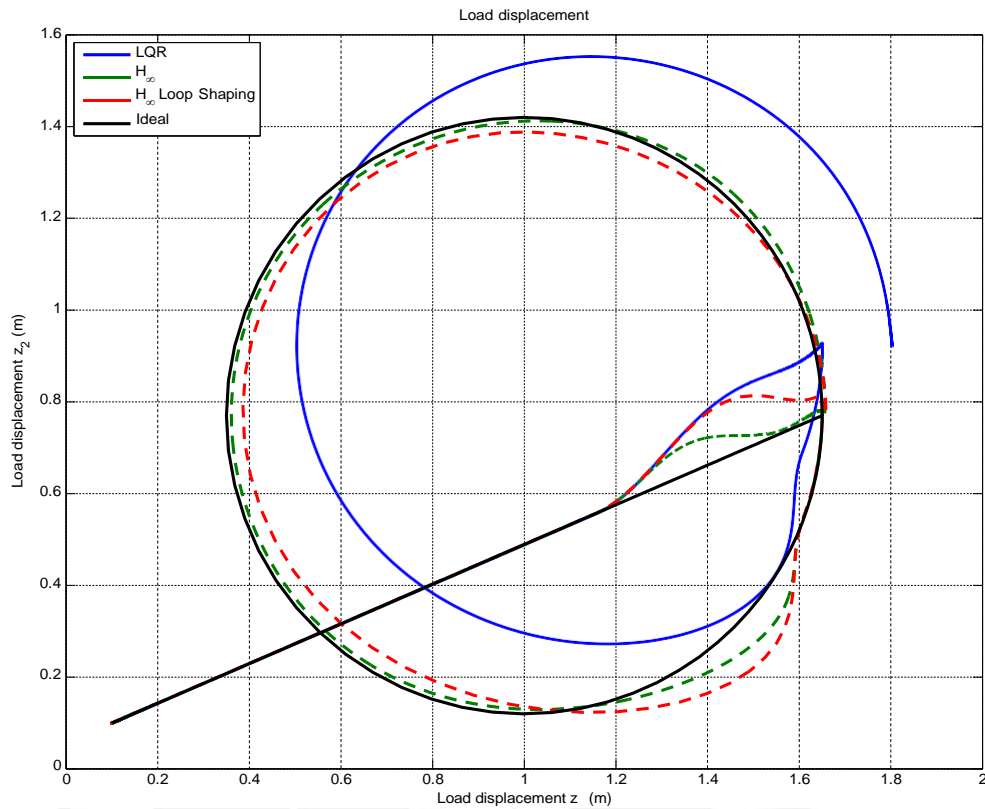
Figure 5.45: Settled Trajectory Load Displacement in z_1-z_2 with LQR.

Control Type	Robustification Type	z_{1_d}	z_{2_d}	z_{3_d}	$z_{1_{sim}}$	$z_{2_{sim}}$	$z_{3_{sim}}$
	-	1.65	0.77	-0.7	1.99	1.11	-0.63
Pole Placement	H_∞	1.65	0.77	-0.7	1.67	0.79	-0.70
	H_∞ Loop Shaping	1.65	0.77	-0.7	1.67	0.79	-0.71
	-	1.65	0.77	-0.7	1.80	0.92	-0.67
LQR	H_∞	1.65	0.77	-0.7	1.66	0.77	-0.69
	H_∞ Loop Shaping	1.65	0.77	-0.7	1.66	0.77	-0.71

Table 5.4: Desired Position of the Payload with disturbances in a Settled Trajectory (*m*).

Finally in Table 5.4 the system with control and robustification presents similar values to the payload in the final position with disturbances. In this case both control strategies can fulfill the required work, Therefore, follow the condition mentioned above, the option to choose is this case is the LQR control with H_∞ Loop Shaping Robustification.

Load Displacement respect to the trolley

Pole Placement
H_∞
H_∞ Loop Shaping

Load displacement z_2 respect to y_c (m)

Load displacement z respect to x (m)

Figure 5.46: Settled Trajectory Load Displacement in z_1-z_2 respect to the Trolley with Pole Placement.

Load Displacement respect to the trolley
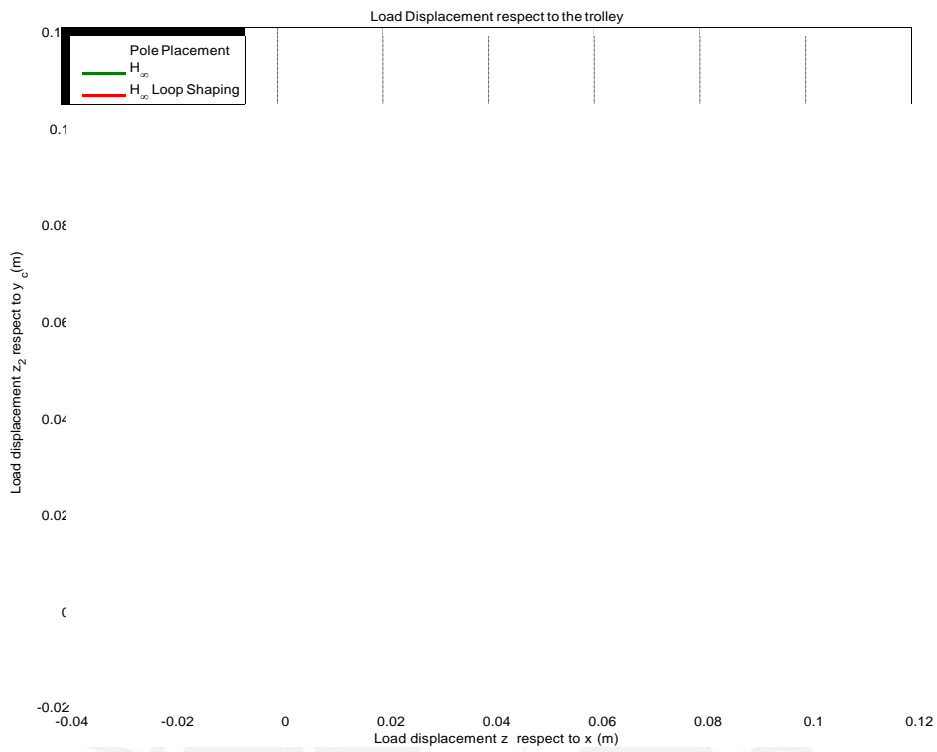
LQR
H_∞
H_∞ Loop Shaping

Load displacement z_2 respect to y_c (m)

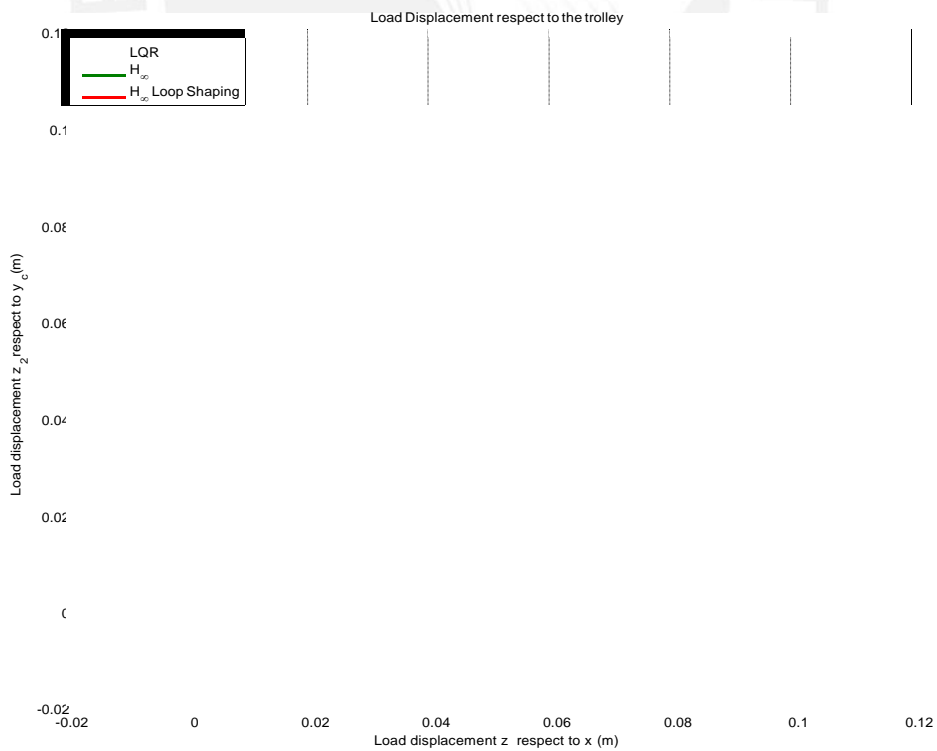Load displacement z respect to x (m)

Figure 5.47: Settled Trajectory Load Displacement in z_1-z_2 respect to the Trolley with LQR.

6 Summary and Outlook

The three dimensional gantry crane has been modeled based on its underactuated first order dynamics, independent of the load mass, where the inputs are the trolley accelerations of the system. The trajectory generated before and after the robustification gives the information to analyze in which cases the movement of the payload show the requirements of stability and sensitivity against internal and external perturbations. In this work, two conditions in the system have been tested. The first one is the system without movement affected through external perturbations. In the second test the system receives a planning trajectory consisting in a displacement to a specific point in straight line with a displacement of the payload. Then a circular trajectory is probed to check the perturbations in a complex trajectory. In the result we can see that both pole placement and LQR may be devised due to controllability. However, external perturbations affect the planned trajectory and makes inaccurate the desire goal. The robustification control counteracts the effects of the sway produced by external perturbation. Related to the natural swing the values obtained present a small oscilation leaving unchanged the displacement. With respect to the external perturbations, step signal was used to simulate this effect at two times points in both angular directions affects the path. The results show that H_∞ loop-shaping control has shown good performance in comparison to the standard H_∞ control, especially, in driving the accelerations in the trolley to adjust its displacement, however both results are close to the final desired position. Finally, all this analysis will be helpfull to choose an adequate control strategy that may be the reference for more studies related with this type of systems.

Bibliography

[AZ09]   Almutairi, Naif B. ; Zribi, Mohamed: Sliding mode control of a three-dimensional overhead crane. In: *Journal of vibration and control* (2009)

[Bar12]   Barrientos, Antonio.: *Fundamentos de robótica.* Madrid : McGraw-Hill, 2012. – ISBN 9788448156367 8448156366

[BI90]   Byrnes, Christopher I. ; Isidori, A: Exact linearization and zero dynamics. In: *Decision and Control, 1990., Proceedings of the 29th IEEE Conference on* IEEE, 1990, S. 2080–2084

[BN92]   Boustany, F ; Novel, Brigitte d'Andrea: Adaptive control of an overhead crane using dynamic feedback linearization and estimation design. In: *Robotics and Automation, 1992. Proceedings., 1992 IEEE International Conference on* IEEE, 1992, S. 1963–1968

[CGZ05]   Chen, Hongjun ; Gao, Bingtuan ; Zhang, Xiaohua: Dynamical modelling and nonlinear control of a 3D crane. In: *Control and Automation, 2005. ICCA'05. International Conference on* Bd. 2 IEEE, 2005, S. 1085–1090

[CL08]   Cho, Hyun C. ; Lee, Kwon S.: Adaptive control and stability analysis of nonlinear crane systems with perturbation. In: *Journal of Mechanical Science and Technology* 22 (2008), Nr. 6, S. 1091–1098

[CLLL08] Cho, Hyun C. ; Lee, Jin W. ; Lee, Young J. ; Lee, Kwon S.: Lyapunov theory based robust control of complicated nonlinear mechanical systems with uncertainty. In: *Journal of Mechanical Science and Technology* 22 (2008), Nr. 11, S. 2142–2150

[Cra14]   Craig, John J.: *Introduction to robotics : mechanics and control.* Harlow : Pearson, 2014. – ISBN 9781292040042 1292040041

[FDDZ03] Fang, Y ; Dixon, WE ; Dawson, DM ; Zergeroglu, E: Nonlinear coupling control laws for an underactuated overhead crane system. In: *Mechatronics, IEEE/ASME Transactions on* 8 (2003), Nr. 3, S. 418–423

[FLMR95] Fliess, Michel ; Lévine, Jean ; Martin, Philippe ; Rouchon, Pierre: Flatness and defect of non-linear systems: introductory theory and examples. In: *International journal of control* 61 (1995), Nr. 6, S. 1327–1361

[FLR91] Fliess, M ; Levine, J ; Rouchon, P: A simplified approach of crane control via a generalized state-space model. In: *Proc. 30th IEEE Control Decision Conf., Brighton*, 1991, S. 736–741

[HPS13] Hilhorst, Gijs ; Pipeleers, Goele ; Swevers, Jan: Reduced-Order Multi-Objective H_∞ Control of an Overhead Crane Test Setup. In: *Proceedings of the 52nd IEEE Conference on Decision and Control*, 2013, S. 770–775

[Isi95] Isidori, Alberto ; Thoma, M. (Hrsg.) ; Sontag, E. D. (Hrsg.) ; Dickinson, B. W. (Hrsg.) ; Fettweis, A. (Hrsg.) ; Massey, J. L. (Hrsg.) ; Modestino, J. W. (Hrsg.): *Nonlinear Control Systems*. 3rd. Secaucus, NJ, USA : Springer-Verlag New York, Inc., 1995. – ISBN 3540199160

[Jah13] Jahn, B.: *Flachheitsbasierter Regelungsentwurf für einen Portalkran mit anschließender Robustifikation durch H∞ loop-shaping*, 2013. – 20 S.

[Kha00] Khalil, H. K.: Universal Integral Controllers for Minimum-Phase Nonlinear Systems, 2000, 490 - 494

[KKS10] Knierim, Karl L. ; Krieger, Kai ; Sawodny, Oliver: Flatness based control of a 3-DOF overhead crane with velocity controlled drives. In: *Mechatronic Systems*, 2010, S. 363–368

[Lee98] Lee, Ho-Hoon: Modeling and control of a three-dimensional overhead crane. In: *Journal of Dynamic Systems, Measurement, and Control* 120 (1998), Nr. 4, S. 471–476

[MMR01] Martin, Philippe ; Murray, Richard M. ; Rouchon, Pierre: Flat systems, equivalence and feedback. Version: 2001. http://link.springer.com/chapter/10.1007/BFb0110377. In: *Advances in the control of nonlinear systems*. Springer, 2001, 5–32

[Oga10] Ogata, Katsuhiko: *Modern control engineering.* 5th ed. Boston : Prentice-Hall, 2010 (Prentice-Hall electrical engineering series. Instrumen- tation and controls series). – ISBN 9780136156734

[PD11] Pop, Cristina I. ; Dulf, Eva H.: *Robust Feedback Lineariza-tion Control for Reference Tracking and Disturbance Rejec-tion in Nonlinear Systems.* INTECH Open Access Publisher, 2011 http://cdn.intechopen.com/pdfs/23252/InTech-Robust_ feedback_linearization_control_for_reference_tracking_and_ disturbance_rejection_in_nonlinear_systems.pdf

[PPB]   POPESCU, Dan ; PETRE, Emil ; BOBAȘU, Eugen: Sborník vědecky`ch prací Vysoké školy báňské-Technické univerzity Ostrava.

[Res02] Respondek, Witold: Introduction to geometric nonlinear control; lin-earization, observability, decoupling. (2002)

[RKS11] Ruppel, Thomas ; Knierim, Karl L. ; Sawodny, Oliver: Analytical Multi-Point Trajectory Generation for Differentially Flat Systems with Output Constraints. In: *18th IFAC World Congress,* 2011

[RPK13] Robenack, Klaus ; Paschke, Fabian ; Knoll, Carsten: Nonlinear control with approximately linear tracking error. In: *Control Conference (ECC), 2013 European* IEEE, 2013, S. 149–154

[Sas99] Sastry, Shankar: *Nonlinear systems: analysis, stability, and control.* Bd. 10. Springer New York, 1999

[SMD]   Souilem, H ; Mekki, H ; Derbel, N: Flatness control of a crane.

[VFC13] Vazquez, Carlos ; Fridman, Leonid ; Collado, Joaquin: Second Order Sliding Mode Control of an Overhead-Crane in the presence of external perturbations. In: *Decision and Control (CDC), 2013 IEEE 52nd Annual Conference on* IEEE, 2013, S. 2876–2880

[XW12] Xiao, Yu ; Weiyao, LAN: Optimal composite nonlinear feedback control for a gantry crane system. In: *Control Conference (CCC), 2012 31st Chinese* IEEE, 2012, S. 601–606

[Yan09] Yang, Jung H.: On the Adaptive Tracking Control of 3-D Overhead Crane Systems. In: *Adaptive Control* (2009), S. 277–306

[YLL14] Yu, Xiao ; Lin, Xianwu ; Lan, Weiyao: Composite nonlinear feedback controller design for an overhead crane servo system. In: *Transactions of the Institute of Measurement and Control* (2014), S. 0142331213518578

[YS11] Yang, Jung H. ; Shen, Shih H.: Novel approach for adaptive tracking control of a 3-D overhead crane system. In: *Journal of Intelligent & Robotic Systems* 62 (2011), Nr. 1, S. 59–80

[ZD98] Zhou, Kemin ; Doyle, John C.: Essentials of robust control. (1998)

[ZPS12] Zavari, Keivan ; Pipeleers, Goele ; Swevers, Jan: Multi-H_∞ controller design and illustration on an overhead crane. In: *Control Applications (CCA), 2012 IEEE International Conference on* IEEE, 2012, S. 670–674

[ZTMS+13] Zaidi, Mohd ; Tumari, Mohd ; Muhammad Salihin, Saealal ; Mohd Riduwan, Ghazali ; Yasmin, Abd W.: H_∞ controller with graphical LMI region profile for Gantry Crane System. (2013)